Report 9, 1987

ANALYSIS OF RESERVOIR ENGINEERING DATA FROM WELL KhG-1 KOLVIDARHÓLL - ICELAND

Rusmawan H.S. Darwis
UNU Geothermal Training Programme
National Energy Authority
Grensásvegur 9
108 Reykjavík
ICELAND

Permanent Address:
PERTAMINA
Directorate of Exploration and Production
Geothermal Division
Jalan Kramat Raya 59
Jakarta
INDONESIA

ABSTRACT

The Kolviðarholl thermal field is located about 30 km east of Reykjavik, just off the main road to Selfoss. The only well in this area was drilled in 1985.

The techniques dealing with interpretation of reservoir engineering data will be presented for well KhG-1. Reservoir and production engineering tools are applied to pressure and temperature logs obtained during warm-up period, after discharge production data, pressure recovery data and pressure and temperature logs obtained. The well may produces two phase mixture of steam and water but the condition is the reservoir is single phase. The temperature and pressure logs clearly illustrate potential feed point and cross-flow between aquifers. The general temperature profile in the area is characterized by a temperature of about 260°C between 1600 m and 1800 m depth. The pressure recovery data gave the permeability thickness of 1.6×10^{-12} m^3 (1.6 Dm). The enthalpy of the discharged is 1475 kJ/kg which means two phase flow during discharge but the compressibility (c_t) is 1.05×10^{-9} Pa^{-1}, its mean single phase flow during shut in.

Having the above result will help to predict the reservoir performance and give production strategy from that well in the future.

TABLE OF CONTENTS

LIST OF TABLES

LIST OF FIGURES

1. INTRODUCTION

This project report was carried out while the author was awarded the United Nations University (UNU) Fellowship to attend the 1987 Geothermal Training Programme at National Energy Authority of Iceland.

The subject of this report is to interpret and in some cases simulate various wellbore measurements carried out in the well KhG-1 in SW - Iceland (Figure. 1). The well is the first and the only one drilled in a high temperature field located on the southern margin of the large geothermal system, Hengill. The Reykjavik District Heating System plants to operate a Geothermal Power Plant under construction in the field and the well is drilled as a final part of a pre-exploration survey.

Various types of tests have been applied in well KhG-1. Downhole temperature and pressure were measured frequently in the well during the warm up period. They are analyzed here in order to estimate the static formation temperature and pressure in the reservoir prior to drilling.

The pressure recovery and production tests were obtained analyze the reservoir behavior. The results obtained from those tests give an idea of the reservoir properties, i.e average value of transmissivity in the drainage well volume, storage and mean reservoir pressure. They can be used to predict the well behavior, i.e to indicate whether as the well is damaged or stimulated and to tell if the shape of reservoir is homogeneous or heterogeneous. They can help in making a decision to drill another well or if this well can produce in the future.

2. WELL KhG-1, KOLVIÐARHOLL GEOTHERMAL AREA

2.1. Location and Drilling of Well KhG-1

The Kolviðarholl geothermal field is located about 30 km east of Reykjavik, just off the main road to the town Selfoss (figure 1). The only well (KhG-1) in this area was drilled from 02-10-1985 to 20-11-1985 with the Dofri rig. The well is 1816 m deep and is designed as follows: 18" casing from 0 to 60 m; 13 3/8" safety casing from 0 to 223.4 m; 9 5/8" production casing from 0 to 773.9 m; and 7" liner from 741 m to 1805 m. Circulation losses were occurred during drilling at depths of 1000 m; 1120 m; 1300 m; 1450 m; from 1550-1560 m and from 1710-1730 m. This indicates that several aquifers were cut by the well.

2.2. Instrumentations

Pressure and temperature measurements were carried out using the Amerada mechanical gauges (Amerada RPG-3 gauges). Description and Operating Instructions 1974 : GRG, Oklahoma, U.S.A.) and are presented on figure 2-3.

2.2.1. Pressure element

The active element in the pressure gauge is a helical Bourdon tube, fixed at one end and free to rotate at the other. The interior of the tube is subjected to the pressure in the well. The resulting rotation of the free end of the Bourdon tube is transmitted directly to a recording stylus without the use of the gears on levers. The stylus records on a metal chart coated on one side with a special paint. The paint renders extremely low friction and makes the scribed lines easily visible. To obtain the maximum accuracy a chart scanner is used to measure the chart deflections. The chart is carried in a removable cylindrical chart holder, the position of which is controlled by a clock.

2.2.2. Temperature element

For the temperature element the pressure is developed inside the Bourden tube, and inside a connecting reservoir at the bottom of the element which is in direct contact with the well fluids, by a volatile liquid. The vapor pressure of the enclosed liquid is directly related to its temperature, making the rotated position of the free end of the Bourdon tube an usable measure of the temperature of the element. This rotation is recorded on the gauge chart as described above.

2.2.3. Limits of accuracy

The repeatability of a properly maintained gauge is better than 0.1 % of full range of the pressure element in use, while the absolute accuracy is 0.2 %. Temperature above 79°C affect the strength of most Bourdon tubes, so calibrations at temperature above this are necessary to maintain the accuracy of the instrument. The sensitivity of the gauge is 0.2 % of the full scale deflection.

The absolute accuracy of the temperature gauge is usually assumed to be 1°C and is related to the calibration and the operation of the instruments. The sensitivity depends on the span of the temperature element and whether the temperature being measured is in the lower or upper part of the span.

2.3. Measurements in well KhG-1

Well KhG-1 was drilled in order to estimate the reservoir conditions and properties of the Vestur Hengill geothermal field. A series of wellbore measurements were therefore carried out, both during the warm up period, during discharge and after shut in. The measurements made are:

a) Temperature, pressure and water level measurements during warm up period (from November, 1985 to August, 1986).
b) Wellhead pressure, massflow and total enthalpy during production (August-November, 1986).
c) Temperature and pressure recovery at 1400 m depth after shut in.
d) Several downhole pressure and temperature logs (November 1986 - February, 1987).

Pressure and temperature logs give important information about reservoir conditions such as location of aquifers, reservoir pressure and temperature variations with depth and heat flow. The repeated pressure logs before and after discharge give the pressure response of the reservoir due to production but also the location of major feedzones. They can give the phase conditions of the reservoir fluid and the fluid in the well, and the performance of the well. The reservoir pressure was about 113 kg/cm^2 at 1400 m (figure 5), and the maximum temperature is about 260°C at 1600-1800 m depth (figure 4).

2.4. Warm up period and discharge

The temperature and pressure data from the warm up period showed that relatively cold water zone extended from 200-700 m depth in the well ($T < 100$°C). These thermodynamic conditions were far from saturation and implied that stimulation methods were necessary to initiate discharge from the well. Therefore the same stimulation technique was applied in the well KhG-1 as has been used to initiate discharge in wells NG-7, NG-10, and NJ-12 at the Nesjavellir field. Air was pumped into well under 30-40 bar pressure from July 30th, 1986 to August 25th, 1986. At 14.00 o'clock on August 25th, 1986 the well was ready to be discharged. Then master valve was fully opened and a piston was lowered into the well until it was 10-20 m below water level. The piston lower then water level in the well. Warmer water could then enter to the well and heat it up to boiling. After 18 cycles of pulling out the piston, water-steam mixture pulsed out of the well, and full discharge was obtained after 20 periods of pulling the piston. The well discharged to the air for about 14 hours, but then the massflow was directed to a silencer.

On November 27, 1986 (Report OS-85100/JHD-56B, November 1985) the well was shut in and the pressure recovery Amerada of the well measured. Pressure instrument was lowered to 1400 m depth and the pressure recorded constantly for two days. The downhole pressure and temperatures were then measured more irregularly until February 2^{nd} 1987, when the measurement program was finally terminated. The data is presented in Table. 1. Pressure and temperature data is also plotted against the elapsed time (Figure 11 and 12).

3. STATIC FORMATION TEMPERATURE

3.1. Theory

The aim of the static formation temperature test is to determine the undisturbed formation temperature at a certain depth in a geothermal well. During drilling, the circulation fluid disturbs the temperature in the vicinity of the well, making the first temperature measurements after completion inaccurate. The method described below was derived from data obtained during the drilling period, but used on data taken during the warm up period of KhG-1 and seems to be applicable.

3.1.1. Brennand method

The Brennand equation which governs the temperature distribution surrounding the wellbore is obviously based on the thermal diffusion theory as following:

$$1/R\ \delta/\delta R\ (R * \delta T/\delta R) = (\rho\ C_p)/K * \delta T/\delta t \qquad (3.1\text{-}1)$$

The initial condition is :

$$T\ (R,0) = T_f \qquad (3.1\text{-}2)$$

The inner boundary condition throughout the circulation time is :

$$T\ (R_w,t) = T_o \qquad (3.1\text{-}3)$$

and after circulation is :

$$(\delta T/\delta R)_{R=Rw} = 0 \qquad 3(3.1\text{-}4)$$

The outer boundary condition is :

$$T\ (\infty,t) = T_f \qquad (3.1\text{-}5)$$

Equation (3.1-1) and its boundary condition (3.1-2) to (3.1-5) are made dimensionless as follows :
non dimensional radius: $r = R/R_w$
non dimensional time: $\gamma = (t/n)$ where: $n = (C_p*\rho*R_w^2)/K$
non dimensional temperature: $\theta = (T_f-T)/(T_f-T_o)$
to become:

$$<(1/r)*(\delta/\delta r)><(r*(\delta\theta/\delta r)> = \delta\theta/\delta\gamma \qquad (3.1\text{-}6)$$

with boundary conditions:

$\theta\ (r,0) = 0$

$\theta\ (\infty,\gamma) = 0$

and during circulation:

$\theta\ (1,\gamma) = 1$

and after circulation has ceased:

$(\delta\theta/\delta r)_{r=1} = 0$

Transforming the problem into the Laplace space, the resulting ordinary differential equation is solved in conjunction with the initial and outer boundary conditions. The solution is:

$$\theta\ (r,s) = B*K_0*(r\sqrt{s}) \qquad (3.1\text{-}7)$$

where B is an unknown constant.

The Laplace transform in equation (3.1-7) can be inverted to give:

$$\theta(r,\gamma) = (B/2\gamma)*e^{-(r2/4\gamma)} \qquad (3.1\text{-}8)$$

which may be rewritten in dimensional form at the wellbore as:

$$T\ (R_w,t) = T_f - [<zn(T_f-T)>*e^{-(n/4t)}*(1/t)] \qquad (3.1\text{-}9)$$

where:

$n = <(C_p*\rho*R_w^2) / K>$ and $z = (B/2)$

If $t=t_c$ is circulation time and time since circulation is õt, equation (3.1-9) becomes:

$$T(R_w,t)=T_f-\langle zn(T_f-T_o)\rangle * e^{-\langle n/4(\Delta t+pt_c)\rangle} * \langle 1/(\Delta t+pt_c)\rangle \quad (3.1\text{-}10)$$

if n « $(\Delta t+pt_c)$, then the equation can be simplified to:

$$T(R_w,t) = T_f - \langle m/(\Delta t+pt_c)\rangle \quad (3.1\text{-}11)$$

where: $m = zn\ (T_f-T_o)$ as a constant.
Therefore a plot of temperature versus $\langle 1/(\Delta t+pt_c)\rangle$ should produce a straight line of slope m and intercept on formation temperature. From the slope m, the formation and the circulation temperatures, it is possible to determine n, and hence the thermal diffusivity $(K/\rho C_p)$ of the formation, it be required.

3.1.2. Horner method

One approach has been to use a Horner plot. The well is cooled for a time tp is the time that formation, at the depth under study,has been exposed to circulating fluid. This would usually be the time since the drill bit passed the particular depth. Then circulation is halted, and the temperature is measured at several times õt afterward. The data plotted on a Horner plot and extrapolated to $\Delta t = \infty$, that is for $(\Delta t+tp)/\Delta t=1$ to obtain an estimate of final temperature.

The validity of the Horner plot is based on the observation that the equation for heat conduction is:

$$(\rho\ \Gamma)\ \delta T/\delta t = K\ \nabla^2\ T \quad (3.1\text{-}12)$$

i.e., the diffusion equation, which is of same form as the pressure transient equation. This governs the cooling and warming of the well provided that conduction is the dominant mechanism of heat transfers. It is not valid at any zone of fluid loss, at any other permeable zone, or if circulation of fluid occurs spontaneously in the wellbore past the depth observation. i.e., temperature is plotted versus $(t+\Delta t)/\Delta t$

3.2. Analysis and Results

The static formation temperature was calculated at three different depths. Based on measurement taken during the warm up period (Table 1) at 1200 m, 1500 m and 1600 m depth. Horner plots was made (Figure 8) and Brennand plots (Figure 9) or T vs $\log <(t+\Delta t)/\Delta t>$ and T vs $<1/(tp+\Delta t)>$.
It can be seen from the temperature less (Figure 4) that internal flow occurs between an aquifer at 1400 m depth and down to an aquifer at about 1700 m depth. Due to this it is only possible to use the temperature loss down to 1400 m depth and the bottomhole temperature to estimate the formation temperature.

In order to get a good estimation of the reservoir temperatures around well KhG-1, some logs were run after the well had discharged. In that case the well was kept open while the measurement was done. After five days of discharge the temperature logs showed cooling above 1200 m depth. The temperature at 1600 m depth was 264°C and the bottomhole temperature was 265°C (Table. 1).

The different between the measured temperatures after discharge and the calculation temperature using the Horner and the Brennands methods are also listed in Table 4. The average difference using the Brennand method between measured and calculated values is +7.3°C, but +3.3°C using the Horner method, when the temperature is measured before discharge. Using the reference temperature as the one measured after discharge the average difference using the Brennands method is -12.3°C but -15.7°C using the Horner method.

The average calculated temperature shows that the Brennand method gives closest result to the real measured static temperature which has smallest (δT)= -12.3°C. Therefore the Brennand calculation is used for further predictions. Brennand equation gives precisely maximum reservoir temperature at a certain depth. For calculating static formation temperature, the Horner equation is more able to be used, because it gives the more accurate result. Linear-linear plot is only capable for a rough value estimation. Actually it will give the result of maximum temperature as seen the extrapolated temperature by using graphs.

4. PRODUCTION TEST

4.1. Theory

The mass flow rate and specific enthalpy of the fluid during the discharging period (draw down), can be estimated by James formula, as following:

$$P_c = D_c^{0.602} (T/72.2)^{2.195} \quad \text{for } 180°C<T<350°C \qquad (4.1\text{-}1)$$

Where P_c is lip pressure (bar); D_c is inside diameter of the critical notch (m) and T is the feed temperature (°C). Equation (4.1-1) has been confirmed in practice James (1984b) for dry saturated steam as:

$$w = 18.72\ (10)^6 * (P_c^{0.96} * D_d^2 / h_o^{1.102}) \qquad (4.1\text{-}2)$$

where: w is flow rate (kg/s); D_d is inside diameter of the pipe (m); h_o is enthalpy of the discharge (kJ/kg), Substituting (4.1-1) into (4.1-2) gives:

$$w = 18.72\ (10)^6 * (D_c^{2.578}/h_o^{1.102}) * (T/72.2)^{2.1072} \qquad (4.1\text{-}3)$$

The liquid water flow rate through a V-notch (90°) weir box is calculated by an empirical equation (ASME, 1971):

$$w_l = 1.3345\ A^{2.475} / v_l \qquad (4.1\text{-}4)$$

where: A is the head of water (m); w_l is the water flow - rate (kg/s); v_l is the water specific volume (m^3/kg)

The steam fraction x at atmospheric conditions is:

$$x = w_s / (w_l+w_s) = (h_o-h_l) / (h_s-h_l) \qquad (4.1\text{-}5)$$

where: w_s is the steam flow rate (kg/s); h_o is the specific enthalpy of the steam+water (kJ/kg); h_l is the liquid water enthalpy (kJ/kg). Assuming that the stagnation, the steam and water mixture enthalpies are equal (4.1-5) and solving for w gives:

$$w = w_l * (h_s-h_l) / (h_s-h_o) \tag{4.1-6}$$

Finally substituting (4.1-4) to (4.1-6) gives for that total massflow rate:

$$w = 1.3345\ A^{2.475} * v_l^{-1} * (h_s-h_l) * (h_s-h_o)^{-1} \tag{4.1-7}$$

The two unknown variables h_o and w can now be determined by solving (4.1-3) and (4.1-7) simultaneously.

4.2. Production interpretation

Three basic parameters were measured at the surface during the production test (the drawdown period); the wellhead pressure P_{wh}, critical lip pressure P_c and head of water in weir box. The diameter of the discharge pipe was 0.161 m. The measured quantities were (Figure 16-17):

P_{wh} = 6.71 bar
P_c = 1.00 bar
A = 0.154 m

The atmospheric pressure at Kolviðarholl is 0.1 MPa, which gives:

v_l	$= 1.044*10^{-3}$	m^3/kg
h_l	= 419.1	kJ/kg
h_s	= 2675.8	kJ/kg
μ_l	$= 2.79*10^{-4}$	Pa.s

The mass flow rate and the discharge enthalpy can be calculate using equation (4.1-7):

$w = 1.3345*(A^{2.475}/v_1)*(h_s-h_1)/(h_s-h_o)$
$w = 1.3345*A^{2.475}/(1.044*10^{-3})*2256.7/(2675.8-h_o)$
$w = 2.885(10)^6*A^{2.475}/(2675.8-h_o)$

(4.1-8) and (4.1-2)

$w = 18.72\ (10)^6*\ (P_c^{0.96} * D_d^2 / h_o^{1.102})$

By subtracting equation (4.1-8) from equation (4.1-2), rearranging the terms we get:
$R_1*(2675.8-h_o) *D_d^2 * P_c^{0.96} - (A^{2.475} * h_o^{1.102}) = 0$
where: $R_1 = 6.489$

From the equation above, the discharge enthalpy and massflow rate can be estimated:

h_o = 1475 kJ/kg
w = 23.3 kg/s

The average discharge enthalpy of the well was 1475 kJ/kg (Figure - 17) which is greater than the enthalpy of the water at the maximum measured temperature in the well (about 260°C). This indicates two-phase flow into the well. The pressure transient analysis for two-phase inflow, should therefore use mixture densities, viscosities and relative permeabilities for evaluation of reservoir parameters, when using pressure drawdown methods.

Dynamic viscosity of the mixture is defined by Grant et.al 1982:

$$1/\mu_t = (k_{rl}/\mu_l) + (k_{rs}/\mu_s) \quad (4.2\text{-}1)$$

the kinematic viscosity by

$$1/\sigma_t = (k_{rl}/\sigma_l) + (k_{rs}/\sigma_s) \quad (4.2\text{-}2)$$

The mixture density

$$1/\rho_t = <1/(h_s-h_l)>*<(h_t-h_l)/\rho_l>+<(h_s-h_t)/\rho_s> \qquad (4.2\text{-}3)$$

$$1/\rho_t = (x/\rho_l) + <(1-x)/\rho_s> \qquad (4.2\text{-}4)$$

$$x = (h_t - h_l)/(h_s-h_l) \qquad (4.2\text{-}5)$$

where: x is the steam fraction; h_t is total discharge enthalpy; H_s is steam enthalpy; h_w is water enthalpy; k_r is the relative permeability.

The enthalpy of the steam-water mixture is given by

$$h_t = <(h_l * k_{rl})/\sigma_l + (h_s * k_{rs})/\sigma_s> * \sigma_t \qquad (4.2\text{-}6)$$

substituting equation (4.2-2) to equation (4.2-6) and rearranging to:

$$\begin{aligned} k_{rl}/k_{rs} &= (\sigma_l/\sigma_s) <(h_s-h_t)/(h_t-h_l)> = \\ &= (\sigma_l/\sigma_s) * <(1-x)/x> \end{aligned} \qquad (4.2\text{-}7)$$

The mixture density can be determined as follows, applying equation (4.2-4) and (4.2-5). The flowing enthalpy h_t = 1475 kJ/kg. From steam table: at 260°C; h_s = 2796.4 kJ/kg; h_l = 1134.9 kJ/kg; ρ_s = 23.7 kg/m^3; ρ_l = 783.9 kg/m^3; μ_l = 104.8*10^{-6} Pa.s; μ_s = 17.9*10^{-6} Pa.s; σ_l = 0.134*10^{-6} m^2/s; σ_s = 0.755*10^{-6} m^2/s.

Thus

$$x = (1475 - 1134.9)/1661.5 = 0.205$$

From equation (4.2-4),

$$\begin{aligned} 1/\rho_t &= (x/\rho_l) + <(1-x)/\rho_s> \\ &= (0.205/23.7) + (0.795/783.9) \end{aligned}$$

and

$$\rho_t = 103.48 \text{ kg/m}^3$$

By using equation (4.2-7)

$$k_{rl}/k_{rs} = (\sigma_l/\sigma_s)*<(1-x)/x>$$
$$= (0.134*10^{-6})/(0.755*10^{-6}) * <(1-0.205)/0.205>$$
$$= 0.69$$

Assuming Grant relative permeability relation, that is k_{rs} + k_{rs} = 1, then k_{rs} = 0.59 and k_{rl} = 0.41

By using equation (4.2-1) and (4.2-2), the dynamic viscosity and kinematic viscosity of the mixture can be calculated;

$$1/\mu_t = (k_{rl}/\mu_l) + (k_{rs}/\mu_s)$$
$$= <0.41/(104.8*10^{-6})>+<0.59/(17.9*10^{-6})>$$

and

$$\mu_t = 2.71 * 10^{-5} \text{ Pa.s} \quad \text{(dynamic viscosity)}$$
$$1/\sigma_t = (k_{rl}/\sigma_l) + (k_{rs}/\sigma_s)$$

and

$$\sigma_t = 2.6*10^{-7} \text{ m}^2/\text{s} \quad \text{(kinematic viscosity)}$$

5. PRESSURE RECOVERY TEST

5.1. The Description of Test

A pressure recovery or pressure build-up test at well KhG-1 was carried out during a three months period. The production lasted from August 25th, to November 27th, 1986. For the first 86 days 132 mm diameter orifice was used but from there off a 101.6 mm orifice was used. On the final day of the production the master valve controlled the flow.

5.2. Pressure Recovery Interpretation

During pressure recovery test, the temperature and pressure can be plotted in a diagram of clayperon. Figure 10 shows measured pressures and temperatures during the recovery at 1400 m depth. Also marked in the figure is the saturation curve. The figure shows that all the measured data lies in the liquid region, hence showing that only liquid water exists at the depth under consideration. This means that when calculations reservoir parameters based on pressure drawdown single phase should be assumed.

5.3. Model Identification

The model identification can be divided into inner boundary, basic behavior and outer boundary, each one influencing each other. By using Automate Computer Program can be determined characteristic shapes and permits identification at dominant flow regime.

5.3.1. Inner boundaries

Early time data is identified as inner boundaries. The pressure transient data is interpreted by plotting the pressure increment (ΔP) versus (Δt) the time from shut in (Figure 14). The inner boundary effect is observed at early time with dominant effects such as wellbore storage, skin, fracture and partial penetration (Gringarten 1985).

Wellbore storage is characterized by the effect of fluid expansion inside the well giving a straight line of unit slope in the diagnostic plot. Figure 14, shows a slope of 1, which indicates that wellbore storage affect the first two hours of the data.

Based on skin effect theory (Gringarten, 1985), if the skin is positive, then the well has a steady state pressure drop but it also indicates that the reservoir is damaged in the walls of the well. On other hand, well KhG-1 has a negative skin, which means the well stimulated. Figure 19, shows that $C_D exp(2S)$ ranges between 10-1000, that's mean well is stimulated or not damaged.
Fractures characteristic will give a straight line on a log-log plot with one half unit slope if the fractures are very permeable or a very low conductivity depended on one quarter the unit slope. Unfortunately the first two hours of the data are dominated by wellbore storage. Therefore fracture effects are not seen in the data. It is however, likely that the well intersects one or more fractures.

5.3.2. Reservoir behavior

Ground water reservoirs are generally divided into two kinds of reservoirs, homogeneous and heterogeneous (Gringarten, 1985). According to figure 18, that shows that ΔP versus Δt in the well KhG-1, the reservoir is homogeneous.
The temperature-pressure profile shows a single medium conductivity affecting the well.

5.3.3. Outer boundary

An outer boundary is indicated from the late time data, either as a no flow boundary or a constant pressure boundary. The log ΔP versus log Δt curve seems to indicates a constant pressure boundary. By using an automate computer program, this result can be determined as a constant pressure boundary (Figure 14-20).

5.3.4. Completed reservoir behavior

Completed reservoir behavior identification is performed on early time data, infinite acting data and late time data. The log-log behavior of the actual reservoir is simply obtained as the super position of the individual log-log behavior of each component of the model representing the reservoir (Gringarten, 1985). Figure 13-20, constructed from a log Δt versus ΔP from the drawdown test in the well KhG-1 shows the wellbore storage performance within homogeneous reservoir behavior and the evidence of constant pressure boundary. It was shown in log-log curve (Figure 14-23). From the inner boundary, infinite acting and outer boundary data shows a well in a homogeneous reservoir which has constant pressure boundary.

5.4. Homogeneous Reservoir Solutions

The basic equation formulated by Earlougher (1977) describes that an isothermal radial flow through an isotropic or homogeneous behavior will follow the equation as below:

$$(\delta^2 P/\delta r^2) + 1/r(\delta P/\delta r) = (\phi \mu c_t/k)(\delta P/\delta t) \qquad (5.4\text{-}1)$$

The equation is basically as the diffusion equation which is assumed that the Darcian flow is slightly compressible throughout a certain thickness will represent a small pressure gradient. The hydraulic diffusivity performs as $(k/\phi c_t \mu)$ converting the solution of diffusivity equation in constant flow rate production will be confirmed as an infinite reservoir. The solution can be displayed as:

$$P_i - P(r,t) = (q\mu/4\pi kh) < -E_i(-\phi c_t \mu r^2/4kt) \quad (5.4\text{-}2)$$

where: E_i = the exponential integral. If the exponential integral < 0.01, the equation can be showed as:

$$-E_i\ (-(\phi c_t \mu r_2/4kt)) \simeq \mathrm{Ln}\ (4kt/\mathrm{Exp}(\Gamma)\phi c_t \mu r^2) \quad (5.4\text{-}3)$$

Substituting (5.4-3) to (5.4-1) and q=wv, the equation can be showed as:

$$P_i - P(r,t) = (wv\mu/4\pi kh)\ \mathrm{Ln}\ (4kt/\mathrm{Exp}(\Gamma)\phi c_t \mu r^2) \quad (5.4\text{-}4)$$

if $r=r_w$, and it produces from all the reservoir thickness with the skin factor consideration, the equation can be:

$$P_{wf} = P_i - (wv\mu/4\pi kh) < \mathrm{Ln}(4kt/\mathrm{Exp}(\Gamma)\phi c_t \mu r_w^2) + 2S \quad (5.4\text{-}5)$$

dimensionless time as:

$$t_D = kt/\phi c_t \mu r_w^2 \quad (5.4\text{-}6)$$

dimensionless radius as:

$$r_D = r/r_w \quad (5.4\text{-}7)$$

the dimensionless pressure can be:

$$P(r_D, t_D) = (2\pi kh/wv\mu)\ <P_i - P(r,t)> \quad (5.4\text{-}8)$$

With the skin factor consideration put into the dimensionless the equation can be:

$$P(1,t_D)+S = P(t_D) + S = (2\pi kh/wv\mu)\ (P_i - P_{wf}) \quad (5.4\text{-}9)$$

substitute equation (5.4-9) into (5.4-5), the equation can be:

$$P(t_D) = 1/2 \text{ Ln } (4kt/\text{Exp}(\Gamma)\phi\mu r_w^2) \qquad (5.4\text{-}10)$$

By using dimensionless time and radius, the equation above can be:

$$P(t_D) = 1/2 \ (\text{Ln } t_D + 0.8091) \qquad (5.4\text{-}11)$$

If equation (5.4-5) would be used for solving practically, the skin factor (S) should not be accounted as seen on equation (5.4-10) and (5.4-11). In case of production the useful equation is diffusivity either as dimensional or dimensionless form. By substituting both equation (5.4-5) & (5.4-11) and based on the superposition theorem obtained formula can be used in total drawdown-build up as the expression following:

$$(P_i-P_{ws})(2\pi k_h/wv\mu) = P_D(t_D+\Delta t_D)-P_D(\Delta t_D) \qquad (5.4\text{-}12)$$

substitute (5.4-12) and (5.4-6), the equation can be:

$$(P_i-P_{ws})(2\pi kh/wv\mu) = 1/2 \ \text{Ln}((t+\Delta t)/\Delta t)) \qquad (5.4\text{-}13)$$

arranging (5.4-13) from Ln type to log type, the equation becomes:

$$(P_i-P_{ws}) = 0.1832(wv\mu/kh) * 1/2 \ \text{Log } ((t+\Delta t)/\Delta t) \qquad (5.4\text{-}14)$$

when pressure is plotted vs $\log(t+\Delta t)/\Delta t$ (Horner method), the result is a straight line with a slope m where:

$$m = 0.1832 \ (wv\mu/kh) \qquad (5.4\text{-}15)$$

To the skin factor (S) can be estimated by substitute equation (5.4-9) and (5.4-14), the equation can be changed as follow:

$$S = 1.1513\ [(P_{ws}(t=1)-P_{wf}(\Delta t=0))/m + ((t_p+1)/t_p) - \log\ (k/\phi c_t \mu r_w^2)) - 0.3513\ ] \qquad (5.4\text{-}16)$$

or can be determined also from (Grant, et. al, 1982, p.285) equation, as following:

$$S = 1.151\ [(\Delta P/m)-\log_{10}\ (kt/\phi\ \mu\ c_t\ r_w^2)+0.251] \qquad (5.4\text{-}17)$$

During pressure recovery test of well KhG-1, the pressure was monitored by running several pressure logs in the well (figure 5). The pivot point was found in the cross flow interval at 1400 m depth. Note that other feed zone at 1000 m, 1300 m, 1450 m, 1525 m, and 1725 m. The feed zone at 1450 m is the most permeable aquifer of the well. The thermal recovery was fast below the pivot point when pumping stopped at the end of drilling.

5.5. Horner Method

The average reservoir pressure can be estimated by Horner method. From figure 15, the late time can be extrapolated to intersects the pressure axis. Then $\log((t+\Delta t)/\Delta t)) \simeq 0$ and $\Delta t \gg t$. The late time straight line can be expressed as:

$$P(\Delta t) = P(\infty) - m\ \log\ ((t+\Delta t)/\Delta t)) \qquad (5.5\text{-}1)$$

So, from figure 15, the average reservoir pressure becomes:

$$P(\infty) = 114.9\ \text{bar}$$

5.6. Homogeneous Reservoir Estimation

Based on the straight line portion of figure. 15 and the equation (5.4-15) above, the transmissivity can be calculated as follows:

$m = 113$ psi/cycle

$= 7.793$ bar/cycle $= 7.793*10^5$ Pa

From chapter 4.2, we can be found:

$v_l = 1.044*10^{-3}\ m^3/kg$

$\mu_l = 2.79*10^{-4}$ Pa.s

$m = 0.1832\ (w\ v\ \mu/kh)$

$kh = 0.1832\ (w\ v\ \mu)\ /m$

$= 0.1832(23.3*(1.044*10^{-3})2.79*10^{-4})/(7.793*10^5)$

$= 1.6*10^{-12}\ m^3$ ---(1.6 Dm) (Permeability thickness)

and

$(kh/\mu_t) = 1.6*10^{-12}\ /\ 2.79*10^{-4}$

$= 5.7*10^{-9}\ m^3/Pa.s$ (Transmissivity)

The storativity can be estimated by (Grant, et. al, 1982, p.285), equation as following:

$$\phi c_t h e^{-2s} = 2.25\ [(kh/\mu)*(t/r^2)*10^{(-\Delta P/m)}]$$

where:

(kh/μ): $5.7 \times 10^{-9}\ m^3/Pa.s$

(t) : 3600 second

(r_w) : 0.108 m

(ΔP) : $39.6*10^5$ Pa

(m) : $7.793*10^5$ Pa

$\phi ch = 2.25*[(5.7*10^{-9})*[3600/(0.108)^2]*10^{-(39.6/7.793)}$

$= 3.2*10^{-8}$ m/Pa

(49 bar $= 2*10^{-9}$ m/Pa)

If porosity and thickness are set to $\phi = 0.1$ and $h = 305$ m the compressibility can be estimated as following:

$c = 3.2*10^{-8}\ /\ (0.1*305)$

$= 1.05*10^{-9}\ Pa^{-1}$

According to Grant. et al., (1982, p.51), who tells about the comparison of the different compressibilities as following:

For single phase: $c_l = 1.2 \times 10^{-9}$ Pa^{-1} (water)

$c_s = 3.0 \times 10^{-7}$ Pa^{-1} (steam)

For two phase : $c_t = 1.4 \times 10^{-6}$ Pa^{-1}

So, $1.05 * 10^{-9}$ Pa^{-1} can be determined as single phase flow in reservoir (1400 m depth).

The skin factor depend on porosity (ϕ), compressibility (c_t) and reservoir thickness (h). Using those equation (5.4-16) or equation (5.4-17), the skin factor value can be calculated:

$$S = 1.151 \; [(\Delta P/m) - \log_{10}(kt/\phi \; \mu c r_w^2) + 0.251] \quad (4.3.3\text{-}17)$$
$$= -0.125$$

S = Skin factor is negative, that its mean the well KhG-1 as the stimulated well or non damaged well (Gringarten, 1985).

The transmissivity value is $5.7*10^{-9}$ m^3/Pa.s obtained based on the pressure recovery test for well KhG-1, and kh is 1.6 Dm that mean is still moderate production, if it compared with kh data from the Nesjavellir field.

5.7. Computerized Calculation

By using the program Automate available in UNU some values of kh (Table 3) were calculated the following method:

- Line source solution (Figure 25)
- Storage and skin (Figure 19, 22 and 26)
- Horner plot (Figure 18, 21 and 24)

Skin effect can be determined by the Horner method and storage & skin. It can be seen clearly based from the early time data. The constant pressure boundary in homogeneous reservoir shown on above of three type curves, which are initiated from figure/chart in the infinite acting time and late time.

The calculated distance between wellbore and a linear boundary is about 200 m, has shown on table 6 and 7 of infinite acting and late time data, but by using the late time data the result seem to be much closer to the condition because the pressure value is obtained through above calculation (P = 114.7 bar) is much closer to the reservoir pressure.

6. DISCUSSIONS

The pressure recovery test was carried out in the well KhG-1 at 1400 m depth. Several kind of measurement had been carried out i.e temperature and pressure in order to obtain a data base. The maximum temperature was measured in 1600 depth shows the temperature of about 260°C and at about 1800 m depth about 262°C. The well KhG-1 is determined that the enthalpy is about 1475 kJ/kg and the temperature of 260°C during discharging. In this test also have been calculated the mixture (steam+water) density, the mixture viscosity, relative permeability for evaluating reservoir parameters. Its used two phase flow equation. The (P versus T) on figure 10, shows that the fluid as a single liquid phase which is in unsaturated condition at the reservoir temperature-pressure. The T-P plot shows that KhG-1 data is located on the left side of the saturation line on the graph T-P. The fluid may flash in the well, but the low enthalpies and steam fraction suggest that the boiling may happen close to the surface or totally on the surface. According calculation where the compressibility (c) = $1.05*10^{-9}$ Pa^{-1} as a single phase flow in reservoir after well shut in.

Figure. 11 shows that the maximum temperature of 260°C was valid only within 60 hours and then the temperature was dropped to 255°C as stable temperature (Figure 11). Even though the well KhG-1 can be considered as moderate production well, because it has a low conductivity and continuous recharged water. Basic on reservoir behavior and its thermodynamic during build up period (Figure 10) show that the hot water may flush either within the wellbore or on the lips of wellhead during discharge.

Cold water zone at the depth interval 800 m - 1000 m may exist in well KhG-1 affecting to a increased temperature on uppermost of the well to perform a high temperature fluxtuation (Figure 6), and Figure. 17, shows the close stable production rate in the well KhG-1. The water flow rate ranges from 9 -11 kg/s within the total massflow of about 23 kg/s at well pressure 7 bar.a. Flowing enthalpy is about 1475 kJ/kg and steam fraction 20.5 % gives the suggestion that KhG-1 may able to be used either for electric generating and direct uses. The stability of the flow rate behavior confirms to the stable at 7 bar.a which is in the smallest changing pressure.

7. CONCLUSIONS AND RECOMMENDATION

The reservoir behavior in well KhG-1 is considered to be a single phase water dominated. Therefore fraction obtained from production was low, although the well produces two phase flow during discharge.

The main reservoir is situated at 1400 m depth with the maximum of 260°C. It seems to be a single feeding zone in the well.

Evaluation of the pressure recovery data obtained from well KhG-1 shows a straight line or a single slope on the semilog graph. It can be interpreted that well as a well having a low conductivity homogeneous reservoir which has a constant pressure boundary.

Static formation temperature is able to obtain from some ways of calculation showing range from 260 - 270°C in the well KhG-1. The Brennand equation was able to predict the reservoir temperature in that well, but was not corrected to predict static formation temperature in each certain depth by using "warm-up period" data of well KhG-1.

ACKNOWLEDGEMENTS

The greatful thanks to Mr. Guðjon Gudmundsson, Mr. Hilmar Sigvaldason, Mr. Guðni Axelsson , Ms.Helga Tulinius, Mr. Benedikt Steingrimsson and the staffs of Borehole Geophysics Section for the excellent guidance during the training period and critically evaluating the work presented in this final report. Also to Mr.Jon Steinar Gudmundsson as The Director of United Nations University, Geothermal Training Programme and his staffs for the excellent organizing of the training programme.

The special thanks are due to all fellows which kept good relation during training in Iceland.

A greatful thank to PERTAMINA (State Oil and Gas Company/ Ministry of Mining and Energy) for the permission to attend the specialized course in Iceland.

NOMENCLATURE

A = Head of water measured at the weir box (m)
B = Formation volume factor = reservoir volume/surface volume
c = Compressibility (1/Pa)
C_p= Specific heat capacity at constant pressure of rock in situ (J/kgK)
C = Wellbore storage (m^3/Pa)
D = Diameter (m)
H = Depth (m)
h = Tickness (reservoir) (m)
h = Specific enthalpy (+ subscript) (kJ/kg)
k = Permeability (m^2)
K_o= Modified Bessel funtion of the second kind of order zero
K = Conductivity of rock in situ (W/mK)
L = Length to sealing fault (m)
m = Slope (psi/cycle)
n = $(C_p \rho R_W^2)/K$ (s)
p = constant
P = Absolute pressure (MPa)
q = Volumetric flowrate (m^3/s)
r = Radial distance (m)
= (R/R_W) non dimensional radius
R = Radius from axis of the wellbore (m)
R_W= Wellbore radius (m)
s = Laplace transform variable (dimensionless)
S = Skin factor (dimensionless)
T = Temperature (°C)
T_o= Circulation temperature (°C)
T_f= Undisturbed formation temperature (°C)
t = Time (s)
V = Concentration of medium (dimensionless)
v = Specific volume (m^3/kg)
w = Mass flow rate (kg/s)
X = Steam fraction (dimensionless)

α = Geometrical factor (dimensionless)

σ = Kinematic Viscosity (Pa.s)

δ = Increment or derivative or distance

μ = Dynamic Viscosity (Pa.s)

ϕ = Porosity (dimensionless)

θ = Temperature=$(T_f-T)/(T_f-T_o)$ (dimensionless)

θ = Laplace transform of temperature (dimensionless)

ρ = Density of rock in situ (kg/m^3)

z = constant

γ = Time = $(K*t)/(\rho C_p R_w^2)$ (dimensionless)

SUBSCRIPTS

o = Stagnation

c = critical

D = Dimensionless

d = Discharge

f = Most permeability

i = Initial

l = Liquid

m = Least permeable media

p = Production

s = Steam

t = Total

x = Intersection

wf = Bottomhole flowing

ws = Bottomhole static

wh = Wellhead

REFERENCES

Agustsson, H., Sveinbjörnsdottir, A.E., Jonsson, G., Gudmundsson, G., Hermansson, G., Friðleifsson, G.O., Gudmundsson, Gi., Dofra, A., and Sigurðsson, O.:"The Kolviðarholl well KhG-1 report," OS-85104/JHD-60B, November-1985 (In Icelandic).

Axelsson, G.: "Reservoir Physics or Mass and Heat Transfer in Hydrothermal Systems," Lectures in United Nations University, Geothermal Training Programme, Reykjavik, Iceland, 1985.

Ambastha, A.K. and Gudmundsson, J.S.:"Geothermal Two-phase Wellbore Flow: Pressure drop correlations and Flow Pattern Transitions," Proceedings Eleventh Workshop on Geothermal Reservoir Engineering, Stanford University, Stanford, California, January 21-23, 1986, SGP-TR-93.

Ambastha, A.K. and Gudmundsson, J.S.: "Pressure Profile in Two-phase Geothermal Wells: Comparison of Field data and Model Calculations," Proceedings Eleventh Workshop on Geothermal Reservoir Engineering, Stanford University, Stanford, California January 21-23, 1986, SGP-TR-93.

..........., 1971: "Fluid Meters, Their Theory and Application," American Society of Mechanical Engineers (ASME), New York, U.S.A.

Brennand, A.W., 1984: "A New Method for The Analysis of Static Formation Temperature Test," Proceedings 6th New Zealand Geothermal Workshop, The University of Auckland, Geothermal Institute, Auckland, New Zealand, 1984.

Earlougher, R.: "Advances in Well Test Analysis, " Monograph Volume 5, SPE of AIME, Dallas, 1977.

Fernando Samaniego, V.: "Reservoir Engineering Concepts," Instituto de Investigaciones Electricas Heber Cinco-Ley, Stanford University, in Handbook of Geothermal Energy, Editors: L.M.Edwards, G.V.Chilinggar, H.H. Rieke III, W.H.Fertl, By Gulf Publishing Company, Houston, Texas, Printed in United State of America, 1982. p.426-470.

Grant, M.A., Donaldson, I.G., and Bixley, P., 1982: "Geothermal Reservoir Engineering," Academic Press, 1982.

Gringarten, A., 1982: "Flow Test Evaluation of Fractured Reservoirs," in Recent Trends in Hydro-geology, Geological Society of America, special paper 189, Editor T.N. Narasimhan, 1982, p.237-263.

Gringarten, A., 1985: "Interpretation of Transient Well Test Data," Developments in Petroleum Engineering-1, Editors R.A. Dawe and D.C. Wilson, Elsevier Applied Science Publishers, 1985, p.133-197.

James, R., 1986: "Lectures on Geothermal Engineering", United Nations University, Geothermal Training Programme, Reykjavik, Iceland, Report 13, 1986.

Lee, J., 1982: "Well Testing," The American Institute of Mining, Metallurgical, and Petroleum Engineers Inc., United States of America.

Stefansson, V. and Steingrimsson, B. 1981: "Geothermal Logging I, An Introduction to Techniques and Flow Pattern Transitions," Reykjavik, Iceland, 1981. p.45-96.

Sanchez, P.U., 1986: "Reservoir and Production Engineering of Well A-18 in The Los Azufres Geothermal Field, Mexico," United Nations University, Report no.9, Reykjavik, Iceland, 1986.

TABLE.1: KOLVIÐARHOLL KhG-1, PRESSURE AND TEMPERATURE DATA

Depth (m)	P1	T1 (C) 85.11.22	P2	T2 (C) 85.12.1	P3	T3 (C) 85.12.19	P4	T4 (C) 86.02.27	P5	T5 (C) 86.07.15	P6	T6 (C) 86.11.27	P7	T7 (C) 86.12.1	P8	T8 (C) 87.02.02
200		28.6		36.2		35.9	3.80	38.1		38.7			4.94		7.71	58.0
300	9.80	53.2		50.5	12.55	47.1	13.72	51.4		53.0			14.56			65.2
400	19.76	60.4		64.9	22.30	65.0	23.64	65.0		64.9		169.0	24.51		27.82	70.0
500	29.63	64.6		70.3	32.28	68.9	33.50	69.6		68.9			33.34			93.8
600	39.33	75.2		82.7	42.20	79.3	43.15	80.6		78.6		193.7	43.26		47.00	119.3
700	49.17	91.6		99.9	51.93	95.4	52.94	96.4		93.6			52.69		56.72	148.3
800	58.91	112.6		130.7	61.30	135.1	62.36	125.9		131.0		219.3	61.17	171.0	65.06	207.5
900	68.24	127.0		173.0	70.24	161.5	71.55	161.0		156.6		233.9	69.58	198.6	73.77	223.8
1000	77.20	172.0		195.0	79.07	188.8	80.16	190.2		185.6		243.1	77.95	232.4	82.09	238.8
1100	86.08	171.2		204.0	87.72	203.4	88.67	207.0		203.3		253.0	86.02	251.3	90.45	247.7.
1200	95.07	171.6		211.2	96.62	218.2	96.99	224.3		221.5		255.5	93.97	254.6	98.57	256.1
1300	104.21	153.9		218.4	104.75	232.6	105.14	241.3		238.3		258.6	101.79	254.5	106.40	269.8
1400	113.36	145.5		217.0	113.31	233.8	113.37	243.5		241.4	92.30	260.1	109.79	255.3	114.34	266.6
1500	122.42	144.0		214.2	121.59	233.7	121.57	245.8		245.0	100.40	258.6	117.53	255.3	122.29	265.1
1600	131.60	144.0		213.2	130.04	234.4	129.57	257.2		258.6	108.50	259.1	125.43	256.0	130.18	264.4
1700	140.88	146.4		216.5	138.22	237.5	138.01	251.5		255.3	116.60	259.4	133.22	256.3	138.16	263.8
1789	149.22	195.8		238.9	145.11	252.3	144.53	267.5		261.8	123.40	255.3	140.22	252.7	144.81	265.3

Table. 2 Kolviðarholl well KhG-1, pressure recovery at 1400 m.

dt (min.)	dt (hours)	(tp+dt) (Hours) (tp=2051)	(t+dt)/dt	temp. (°C)	pressure (bar)	(psi)
0.0	0.00	well	closed			
26.5	0.44	2051.44	4641.27	260	72.5	1051
29.0	0.48	2051.48	4247.38	260	74.3	1077
31.5	0.53	2051.53	3907.67	260	75.5	1095
34.0	0.57	2051.57	3618.28	260	76.5	1109
36.5	0.61	2051.61	3374.36	260	77.6	1125
39.0	0.65	2051.65	3156.38	260	78.4	1137
41.5	0.69	2051.69	2964.87	260	79.3	1142
44.0	0.73	2051.73	2799.09	260	80.0	1160
46.5	0.78	2051.78	2647.45	260	80.8	1172
49.0	0.82	2051.82	2511.40	260	81.4	1180
52.0	0.87	2051.87	2366.63	260	81.9	1188
57.0	0.95	2051.95	2159.95	260	82.6	1198
62.0	1.03	2052.03	1986.48	260	83.8	1215
67.0	1.12	2052.12	1837.17	260	84.5	1225
72.0	1.20	2052.20	1710.17	260	85.3	1237
77.0	1.28	2052.28	1599.60	260	86.0	1247
82.0	1.37	2052.37	1501.37	260	86.6	1256
87.0	1.45	2052.45	1415.48	260	87.4	1267
92.0	1.53	2052.53	1338.90	260	88.1	1277
97.0	1.62	2052.62	1269.40	260	88.8	1288
102.0	1.70	2052.70	1207.47	260	89.3	1295
107.0	1.78	2052.78	1151.31	260	90.0	1305
112.0	1.87	2052.87	1099.55	260	90.5	1312
117.0	1.95	2052.95	1052.79	260	91.0	1320
122.0	2.03	2053.03	1009.85	260	91.6	1328
127.0	2.12	2053.12	969.82	260	92.0	1334
132.0	2.20	2053.20	933.27	260	92.3	1338
152.0	2.53	2053.53	810.71	260	94.3	1367
335.0	5.58	2056.58	368.37	260	100.0	1450
355.0	5.92	2056.92	347.63	260	100.6	1459
375.0	6.25	2057.25	329.16	260	101.1	1466
415.0	6.92	2057.92	297.52	260	101.6	1473
458.0	7.63	2058.63	269.70	260	102.1	1480
499.0	8.32	2059.32	247.60	260	102.6	1488
540.0	9.00	2060.00	228.89	260	102.9	1492
581.0	9.68	2060.68	212.81	260	103.3	1498
623.0	10.38	2061.38	198.53	260	103.6	1502
684.0	11.40	2062.40	180.91	260	103.9	1507
745.0	12.42	2063.42	166.18	260	104.3	1512
806.0	13.43	2064.43	153.68	260	104.6	1517
868.0	14.47	2065.47	142.77	260	104.9	1521
929.0	15.48	2066.48	133.47	260	105.1	1524
1052.0	17.53	2068.53	117.98	260	105.5	1530
1175.0	19.58	2070.58	105.73	260	105.9	1536
1298.0	21.63	2072.63	95.81	260	106.2	1540
1421.0	23.68	2074.68	87.60	260	106.4	1543
1544.0	25.73	2076.73	80.70	260	106.7	1547
1667.0	27.78	2078.78	74.82	260	106.9	1550
1755.0	29.25	2080.25	71.12	260	107.0	1552
1815.0	30.25	2081.25	68.80	260	107.1	1553
1837.0	30.62	2081.62	67.99	260	107.2	1554
1959.0	32.65	2083.65	63.82	260	107.3	1556
2081.0	34.68	2085.68	60.14	260	107.5	1559
2203.0	36.72	2087.72	56.86	260	107.7	1562
2325.0	38.75	2089.75	53.93	260	107.7	1562
2447.0	40.78	2091.78	51.29	260	107.9	1565
2569.0	42.82	2093.82	48.90	260	108.1	1567
2691.0	44.85	2095.85	46.73	260	108.1	1567
2813.0	46.88	2097.88	44.75	260	108.3	1570
2936.0	48.93	2099.93	42.91	260	108.4	1572
3060.0	51.00	2102.00	41.22	260	108.5	1573
4700.0	78.33	2129.33	27.18	255	109.7	1591
4725.0	78.75	2129.75	27.04	255	110.1	1596
14685.0	244.75	2295.75	9.38	255	110.4	1601
27412.0	456.87	2507.87	5.49	255	111.0	1610
95160.0	1585.83	3636.83	2.29	255	112.1	1625

TABLE 3 : AUTOMATE RESULT

Parameter	Data type (times)	Time (sec.)	rw (m)	u	kh (mdft)	kh (m+3)	s	C (m3/Pa)	Pwf (bar)	Pi (bar)	m (bar/cle)	kh/u m3/Pa.s	øch m/Pa	ct 1/pa
	Early	3.6e+03	0.108	2.8e-04	785	2.394e-13	-	-	72.50	-	-	8.55e-10		-
LINE SOURCE	All	3.6e+03	0.108	2.8e-04	1017	3.100e-13	-	-	91.60	-	-	1.11e-09		-
	Late	3.6e+03	0.108	2.8e-04	2631	8.899e-13	-	-	101.60	-	-	3.18e-09		-
	Early	3.6e+03	0.108	2.8e-04	1235	3.770e-13	-2.417	-	72.50	139.31	15.32	1.35e-09	3.00e-08	9.8e-10
HORNER	All	3.6e+03	0.108	2.8e-04	3503	1.068e-12	1.916	-	91.60	116.76	5.40	3.83e-09	8.20e-08	2.7e-09
-	Late	3.6e+03	0.108	2.8e-04	5395	1.645e-12	-4.383	-	101.60	114.07	3.51	5.29e-09	1.60e-06	5.2e-08
	Early	3.6e+03	0.108	2.8e-04	1374	4.189e-13	-1.954	0.365	72.50	-	-	1.50e-09		-
STORAGE & SKIN	All	3.6e+03	0.108	2.8e-04	3561	1.086e-12	2.099	1.380	91.60	-	-	3.88e-09		-
	Late	3.6e+03	0.108	2.8e-04	5504	1.289e-12	-4.612	28.410	101.90	-	-	4.60e-09		-

Table. 4 Comparison temperature calculation.

DEPTH	1200 m			1500 m			1600 m		
	Plot	before	after	Plot	before	after	Plot	before	after
tc(minutes)	12510			9270			8190		
Tmax. (°C)		222	256		245	265		259	264
	(°C)	dT(°C)	dT(°C)	(°C)	dT(°C)	dT(°C)	(°C)	dT(°C)	dT(°C)
Lin-lin	224	2	-32	245	0	-20	259	0	-5
Horner	227	5	-29	250	5	-15	259	0	-5
Brennard	229	7	-27	255	10	-10	264	5	0

Table. 5 KhG-1 /Early data by using automate.

DATE OF TEST	25-08-1986	MAIN DATA FILE	darwisrl.mai
TYPE OF TEST	Build-up	PRESSURE DATA FILE	darwisrl.prs
DIAGNOSTIC FILE	darwisrl.dia	RATE DATA FILE	darwislr.flr

WELLBORE RADIUS, ft	0.354	Ct, 10 ^-6/psi	10
FORMATION THICKNESS, ft	1000	VISCOSITY, cp	0.1
Bo, RB/STB	1	POROSITY	5e-2
P/O DIS.,ft (Intf)		Tprod, hrs (optnl)	2051

k, md	1.225	+- 0.1195	Skin	-2.393	+- 0.2371
c, bbl/psi	0.3251	+- 0.1373	Pi, psi	2036	
Xf, ft	89.72		Lin Bndy, ft	90.25	
Bndy Rad, ft	163.9		phicth (Intf)		
Omega			Lambda	1.34e-5	

Table. 6 KhG-1 /All data by using automate.

DATE OF TEST	25-08-1986	MAIN DATA FILE	darwislr.mai
TYPE OF TEST	Build-up	PRESSURE DATA FILE	darwislr.pre
DIAGNOSTIC FILE	darwislr.dia	RATE DATA FILE	darwislr.flr

WELLBORE RADIUS, ft	0.354	Ct, 10 ^-6/psi	10
FORMATION THICKNESS, ft	1000	VISCOSITY, cp	0.1
Bo, RB/STB	1	POROSITY	5e-2
P/O DIS.,ft (Intf)		Tprod, hrs (optnl)	2051

k, md	3.513	+- 0.3801	Skin	1.959	+- 0.9223
c, bbl/psi	1.371	+- 0.122	Pi, psi	1693	
Xf, ft	42.93		Lin Bndy, ft	535	
Bndy Rad, ft	221		phicth (Intf)		
Omega			Lambda		

Table. 7 KhG-1 /Late data by using automate.

DATE OF TEST	25-08-1986	MAIN DATA FILE	darwis55.mai
TYPE OF TEST	Build-up	PRESSURE DATA FILE	darwis55.prs
DIAGNOSTIC FILE	darwis55.dia	RATE DATA FILE	darwislr.flr

WELLBORE RADIUS, ft	0.354	Ct, 10 ^-6/psi	10
FORMATION THICKNESS, ft	1000	VISCOSITY, cp	0.1
Bo, RB/STB	1	POROSITY	5e-2
P/O DIS.,ft (Intf)		Tprod, hrs (optnl)	2051

k, md	5.373	+-	1.365	Skin	-4.392	+-	2.376
c, bbl/psi	27.52	+-	44.44	Pi, psi	1655		
Xf, ft	166			Lin Bndy, ft	579.9	+-	6.756
Bndy Rad, ft	405			phictb (Intf)			
Omega				Lambda			

Björnsson et al.

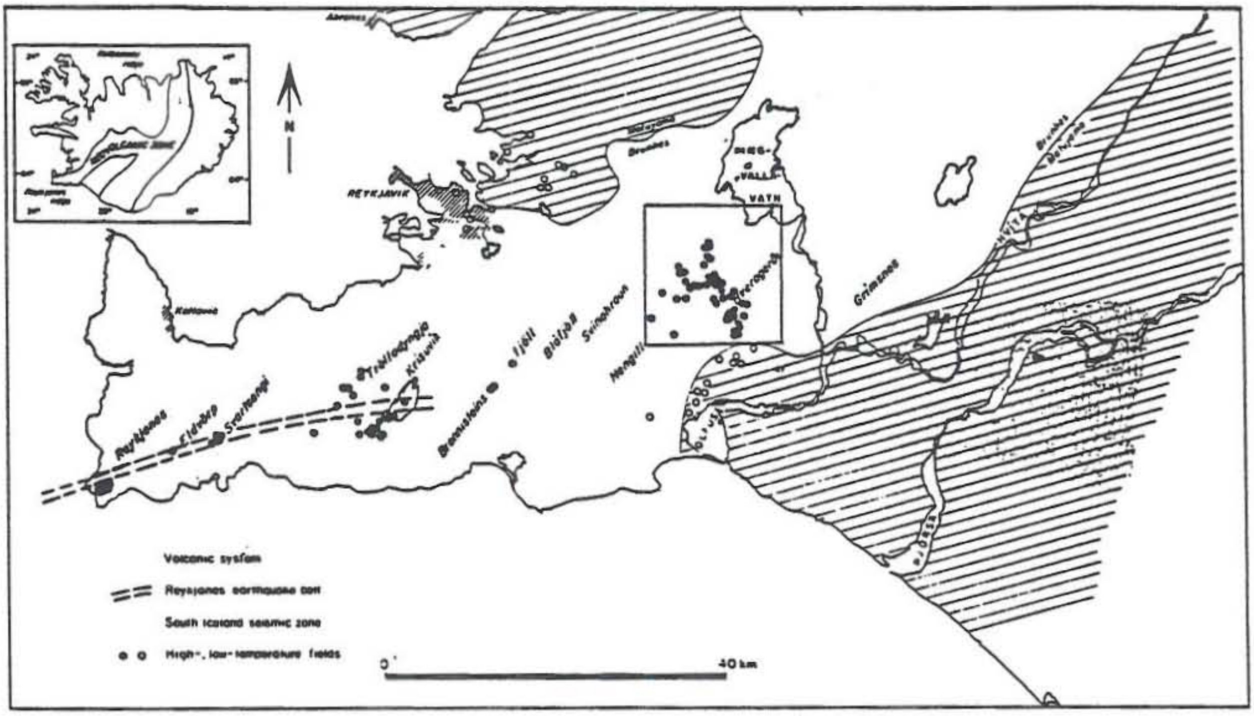

Figure 1. Simplified tectonic map of SW-Iceland and location of the Hengill area. The Neo-volcanic zone is within the Brunhes-Matuyama boundaries. , Earthquake zone (Klein et al., 1977: Einarsson and Björnsson, 1979), volcanic systems (Saemundsson, 1978), and geothermal fields are shown. The Hengill geothermal area is within the square.

Figure. 1 Vestur Hengill (Kolviðarholl Geothermal) area.

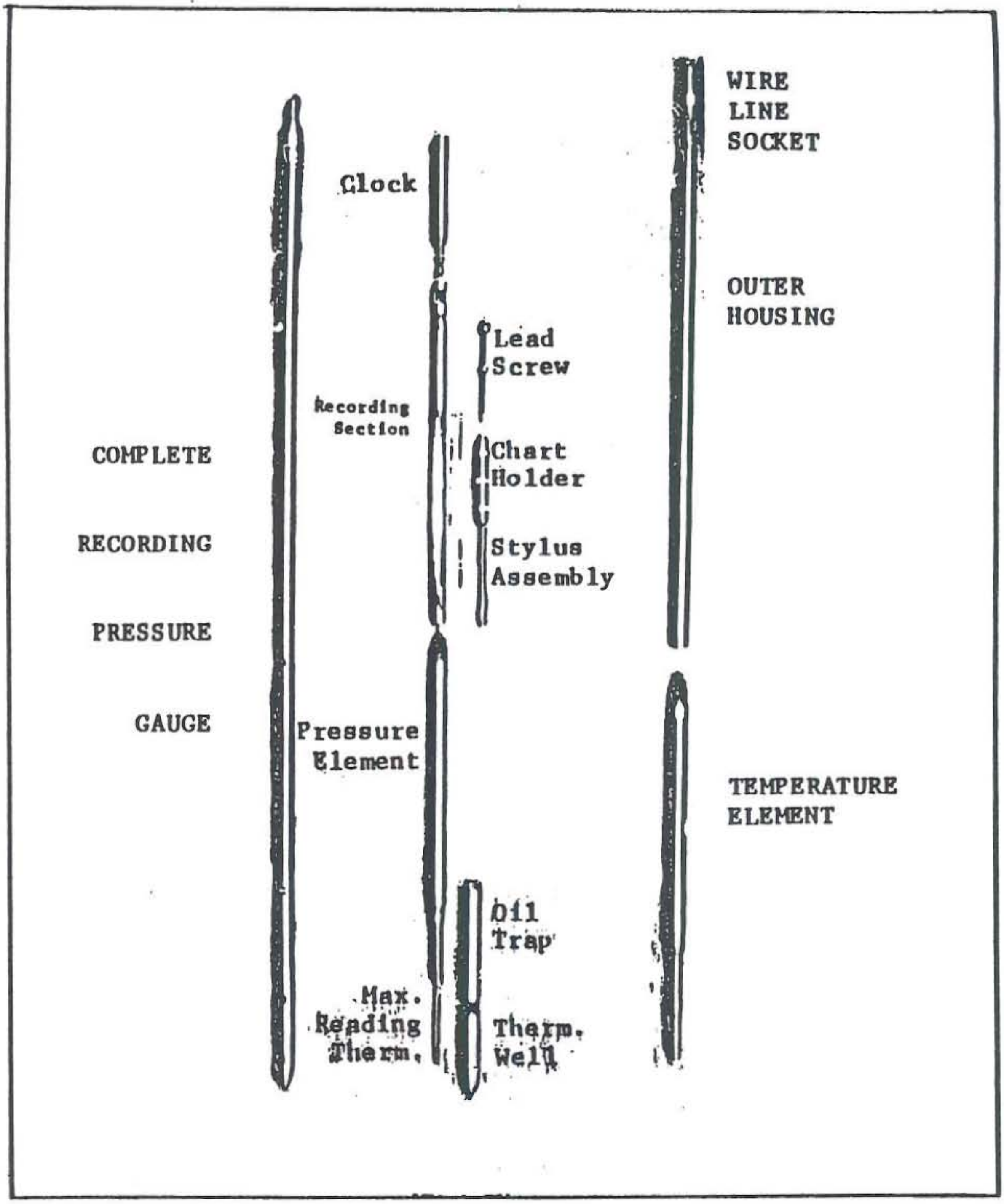

BOTTOM HOLE RECORDING

PRESSURE OR TEMPERATURE GAUGE

RPG-3 1 ¼" Dia. RPG-4 1" Dia.

Figure. 2 Amerada recording gauges for pressure and tempetrature.

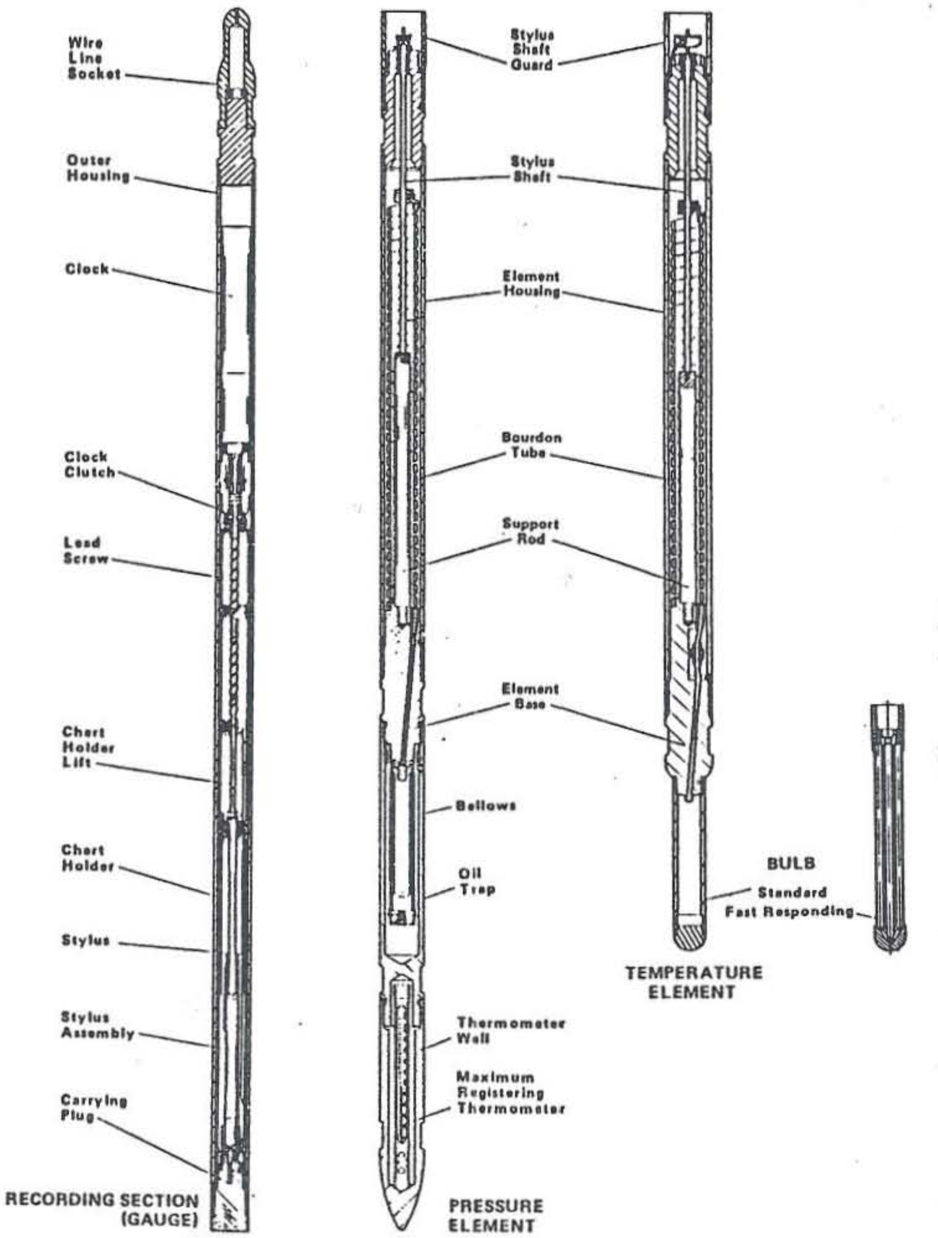

Figure. 3 Cross sections of Amerada pressure and temperature.

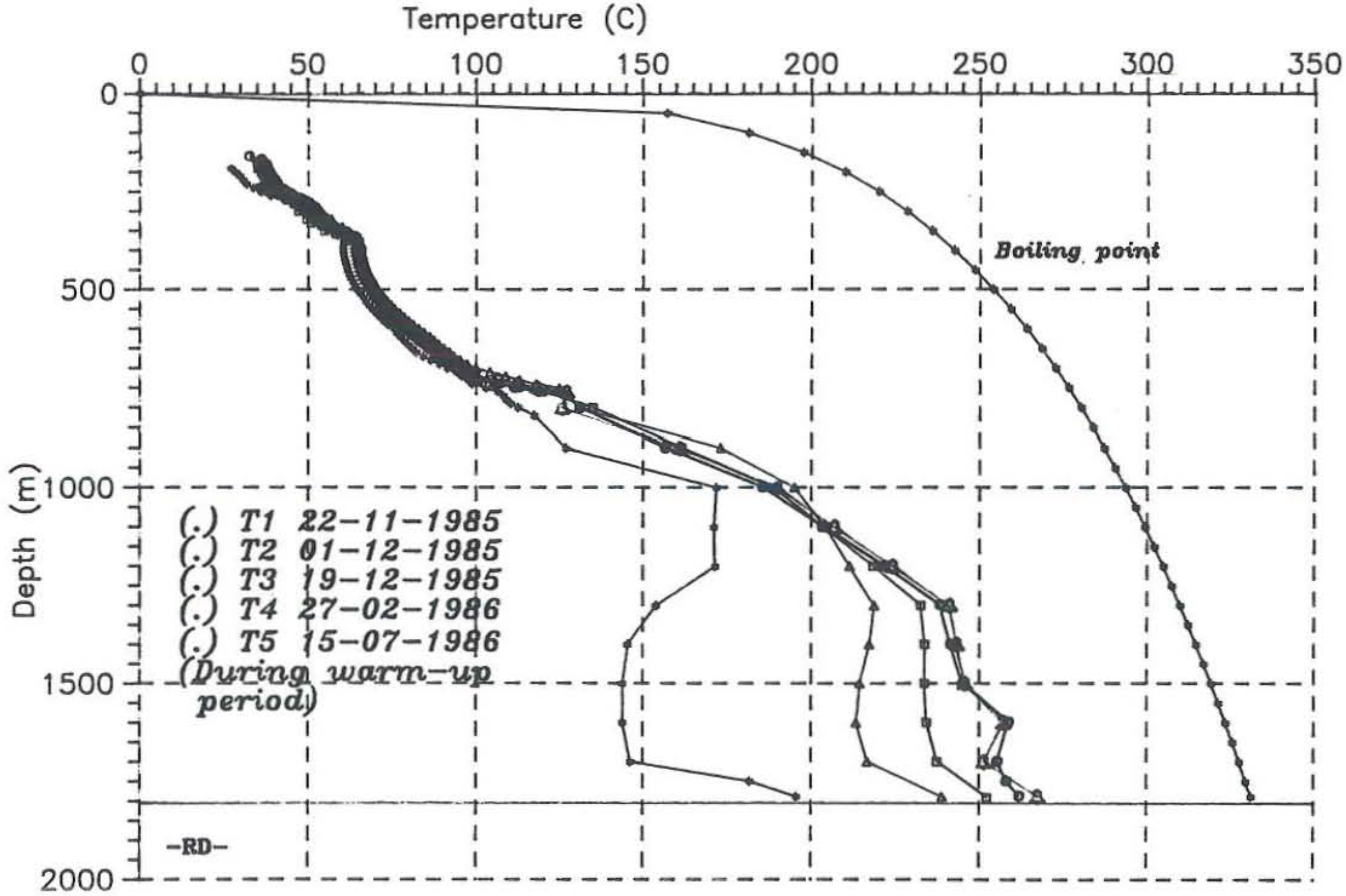

Figure. 4 Kolviðarholl KhG-1. Temperature 1,2,3,4 and 5 profiles.

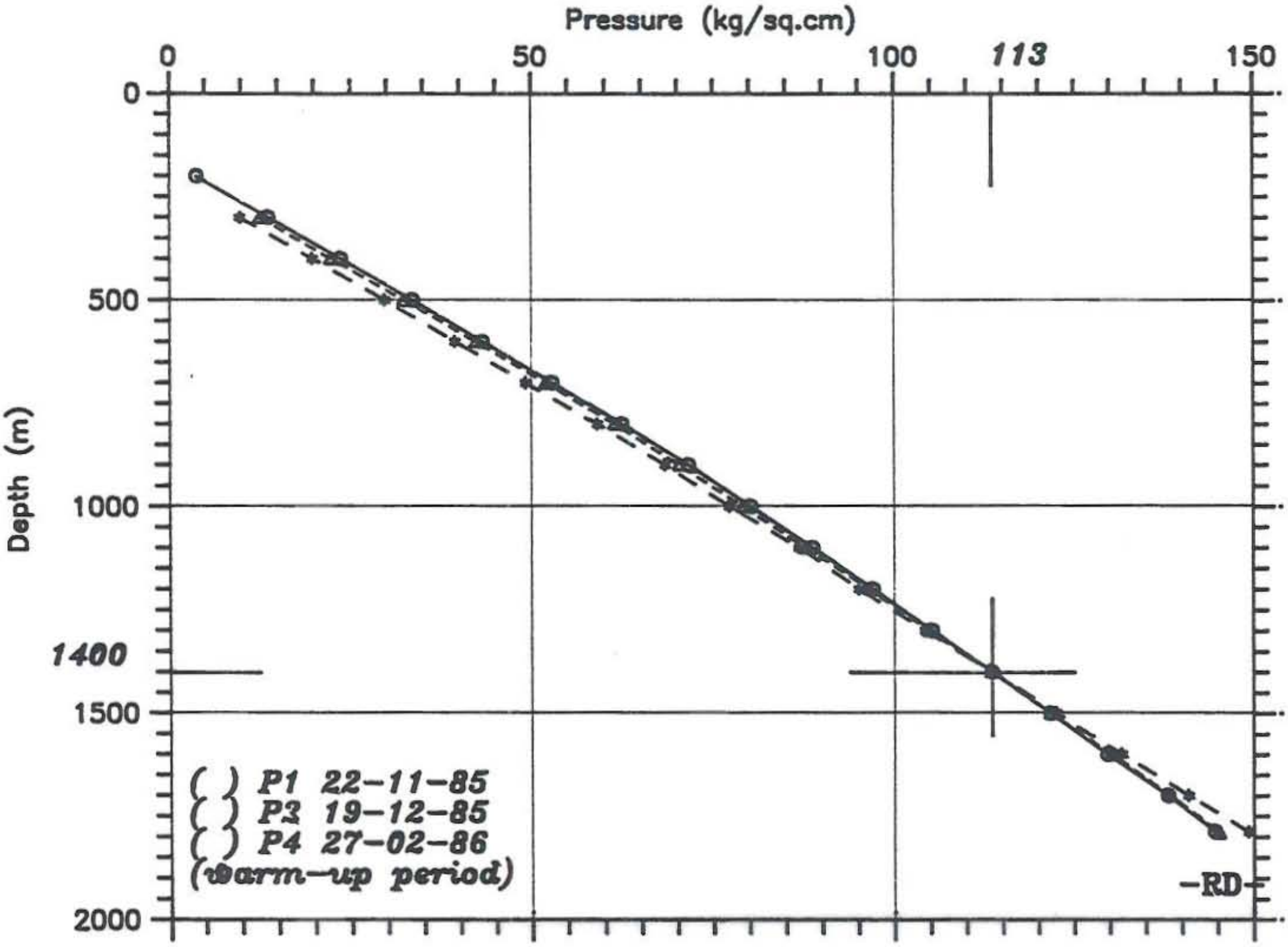

Figure. 5 Kolviðarholl KhG-1. Pressure 1,3 and 4 profiles.

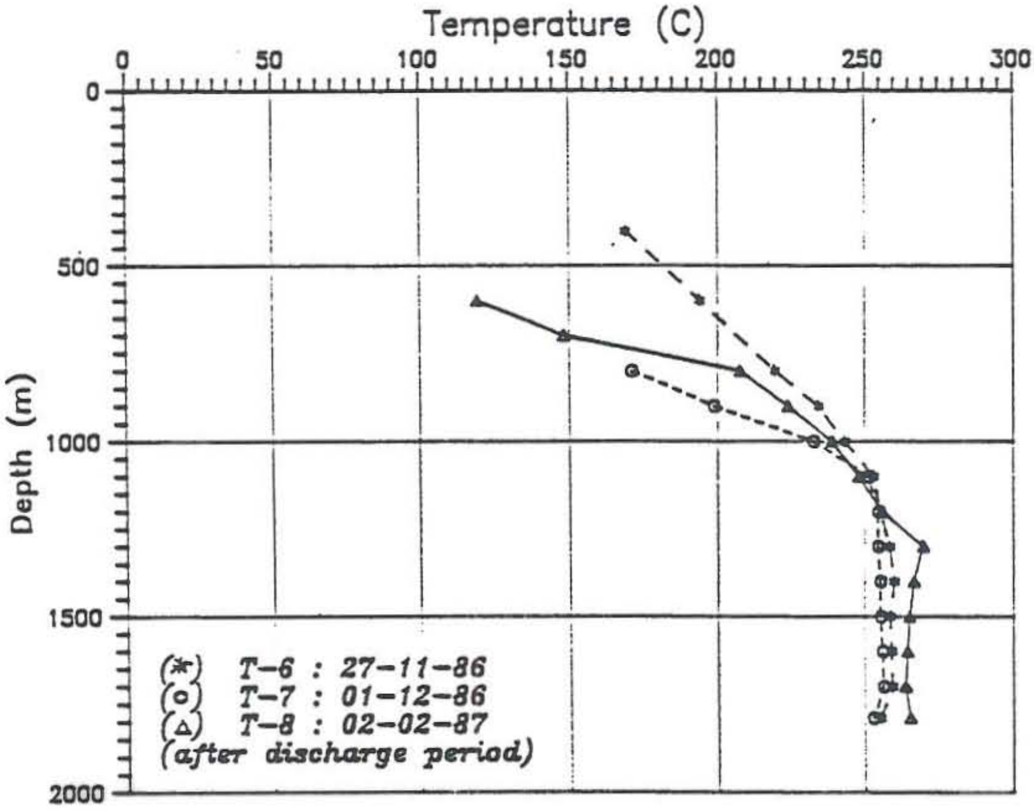

Figure. 6 Kolviðarholl KhG-1. Temperature 6,7 and 8 profiles.

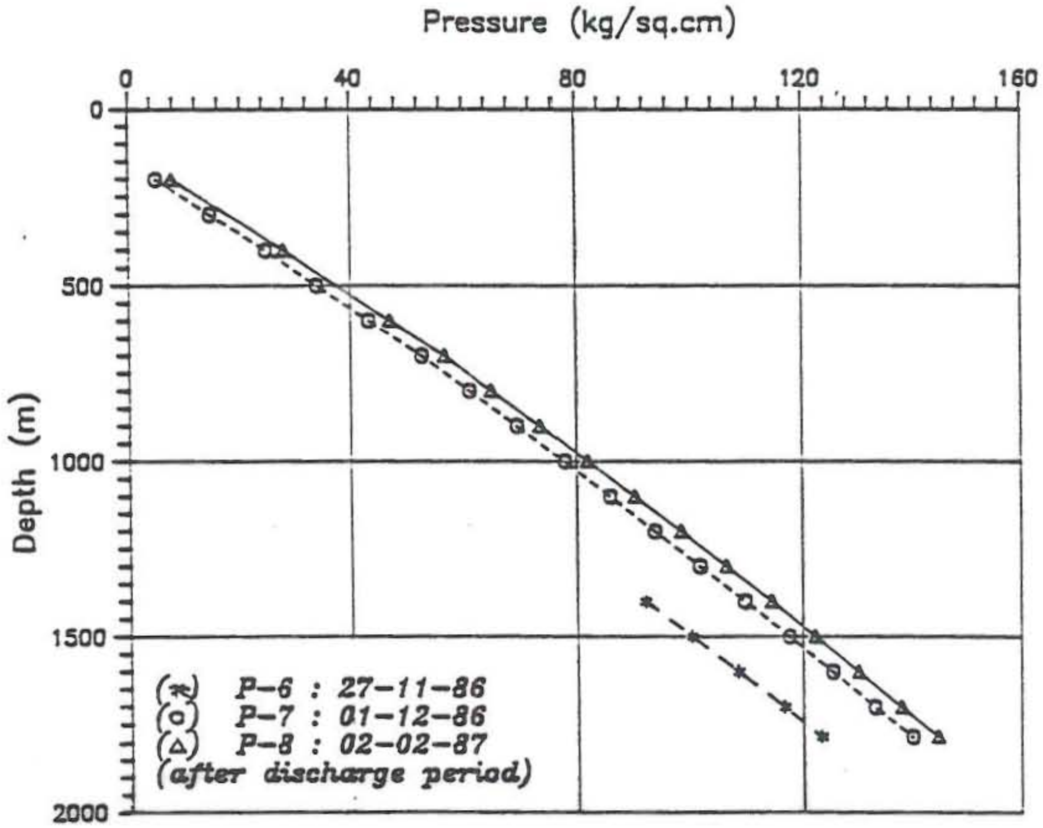

Figure. 7 Kolviðarholl KhG-1. Pressure 6,7 and 8 profiles.

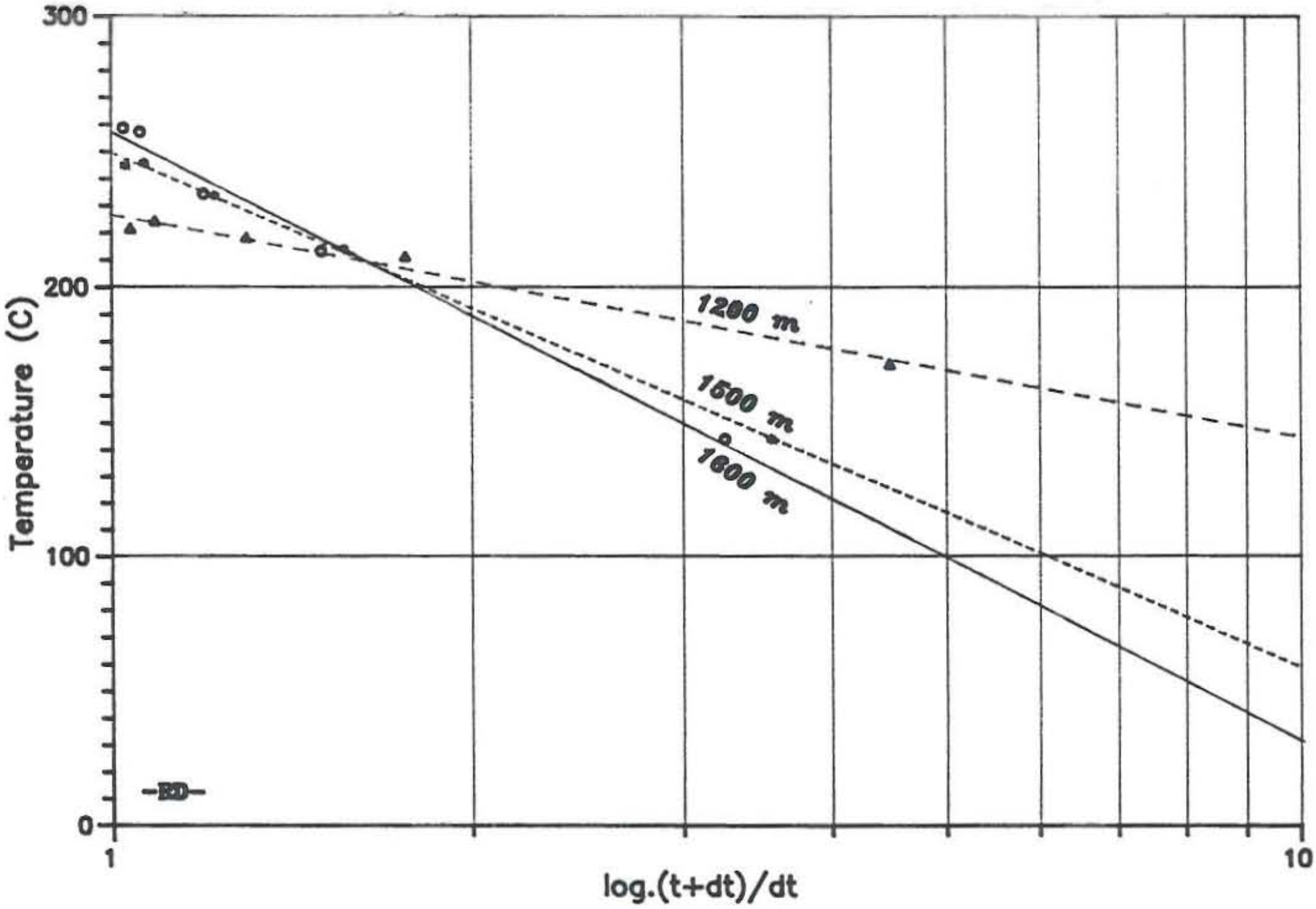

Figure. 8 Temperature profile KhG-1 (Horner plot) at 1200 m, 1500 m, 1600 m.

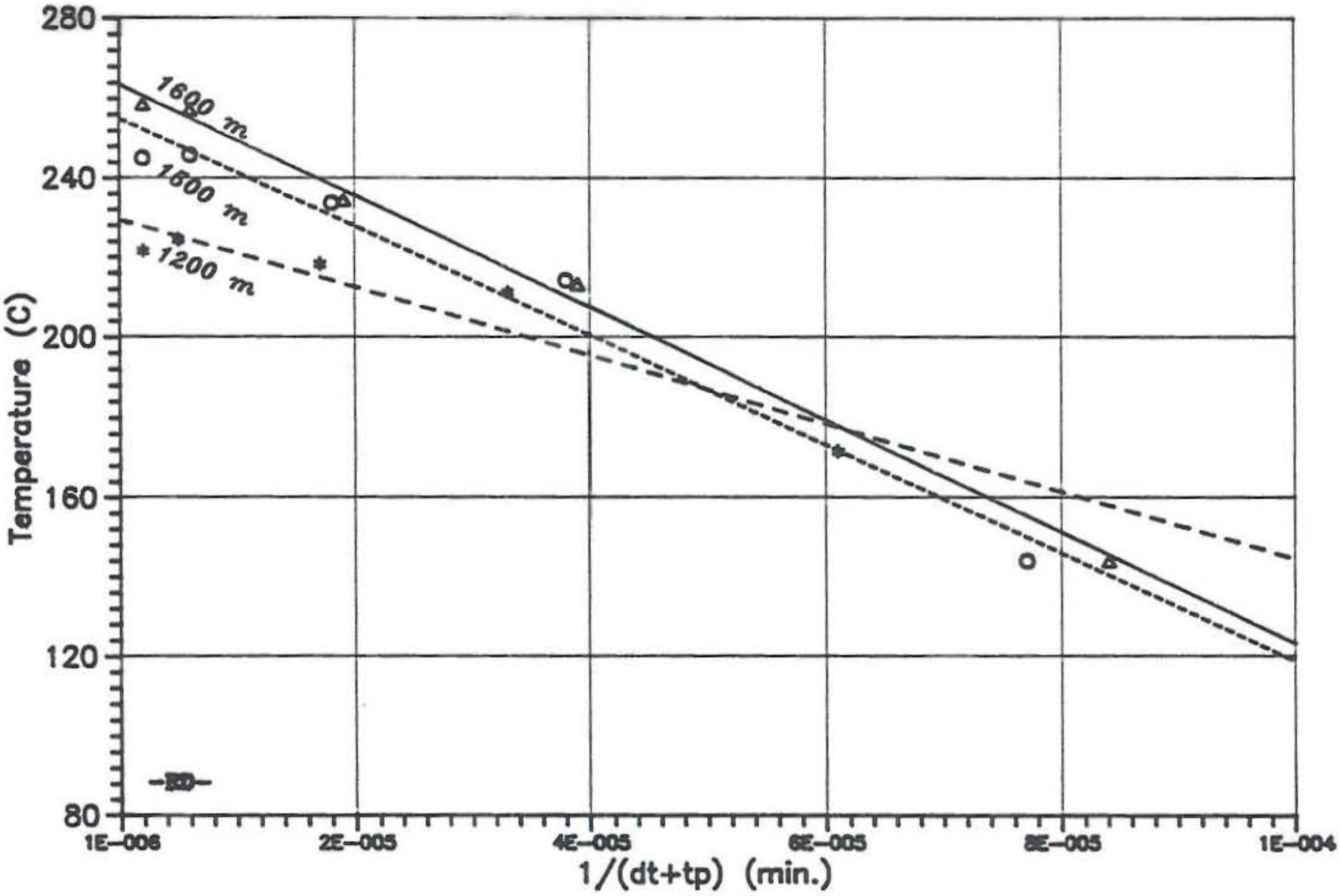

Figure. 9 Kolviðarholl KhG-1, T Vs time inverse-function;
1200 m, 1500 m, 1600 m.

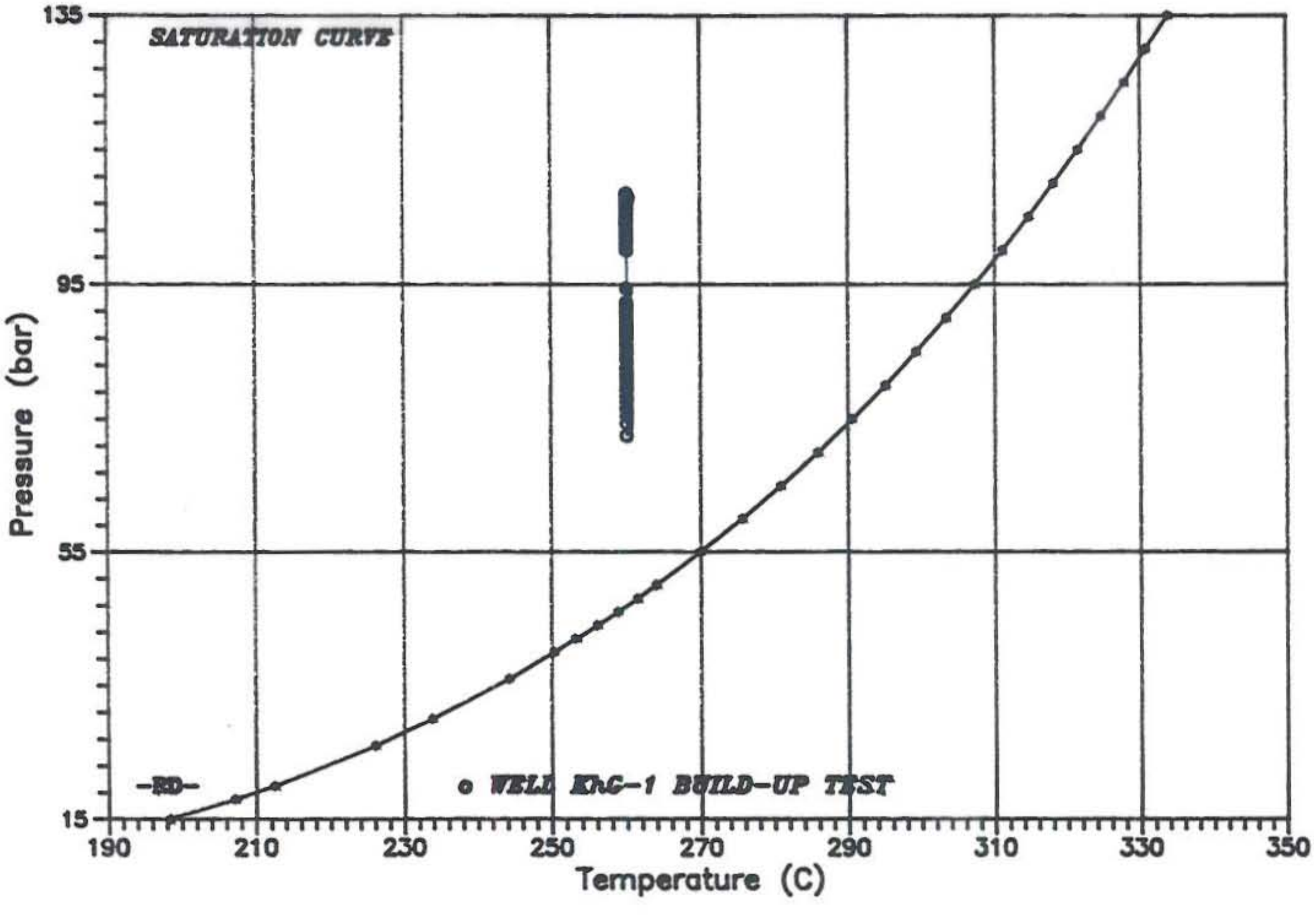

Figure. 10 Thermodynamic bottomhole state behavior during build-up.

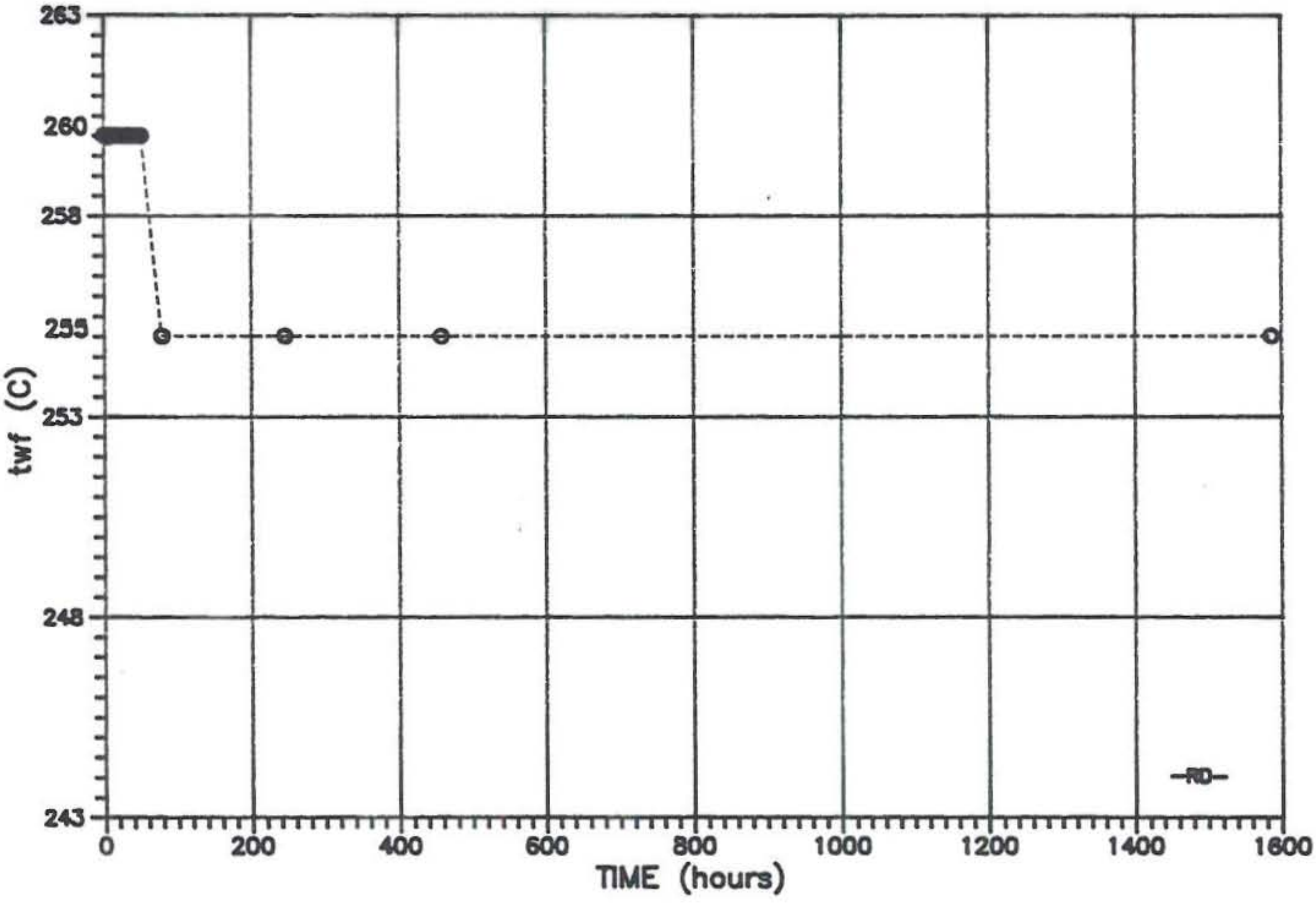

Figure. 11 Temperature build-up behavior.

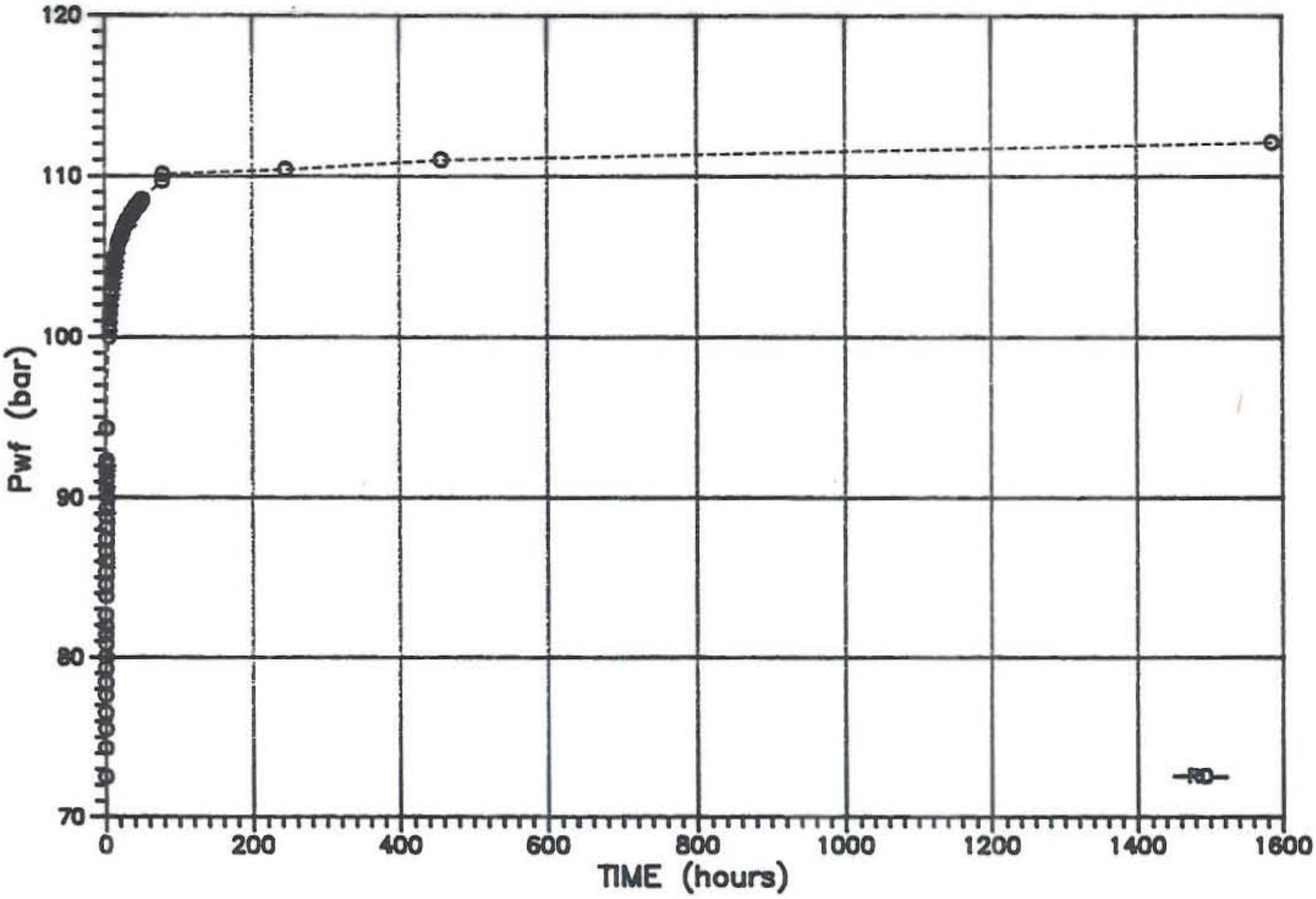

Figure. 12 Pressure build-up behavior.

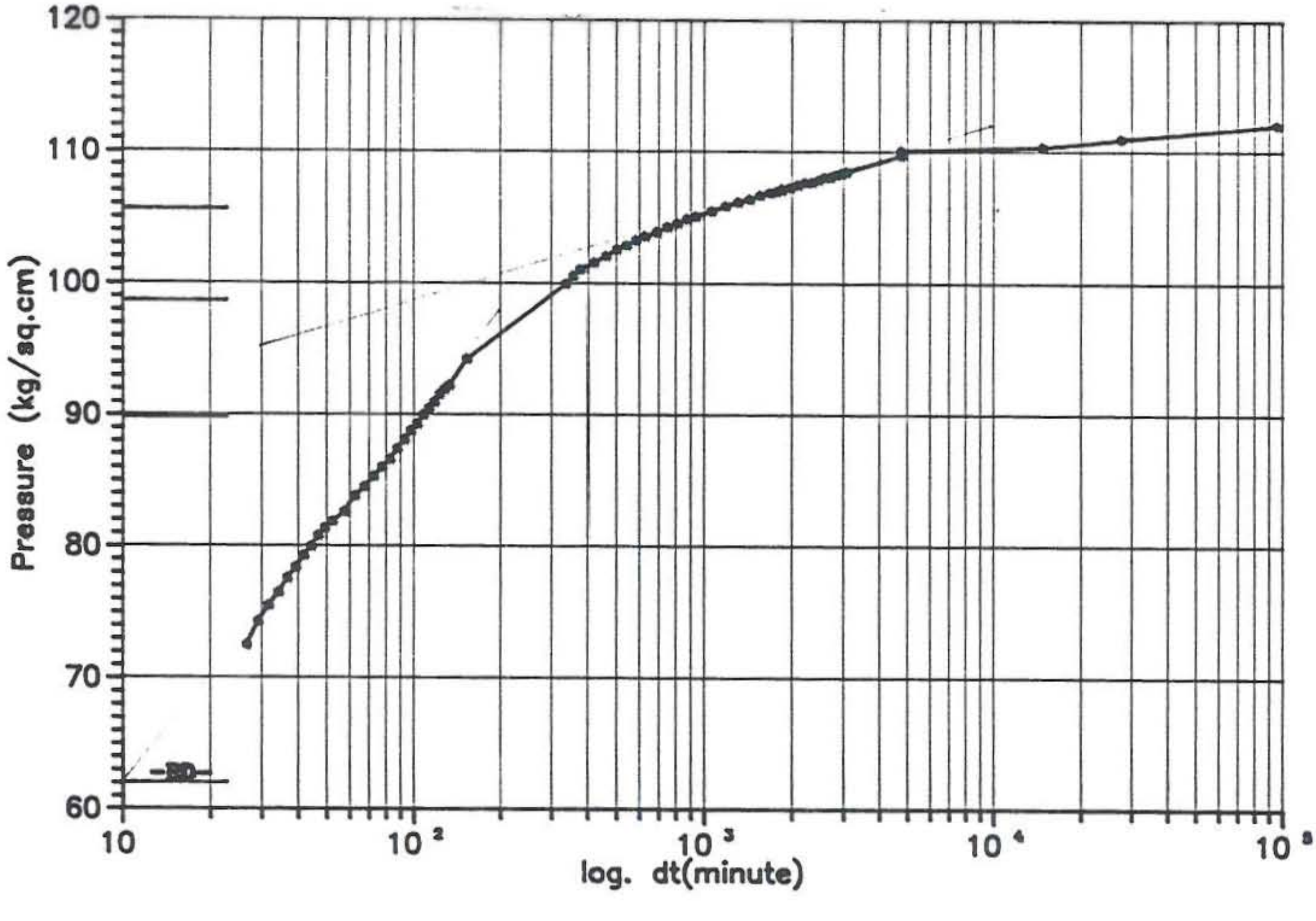

Figure. 13 Pressure recovery KhG-1, on semilog scale at 1400m.

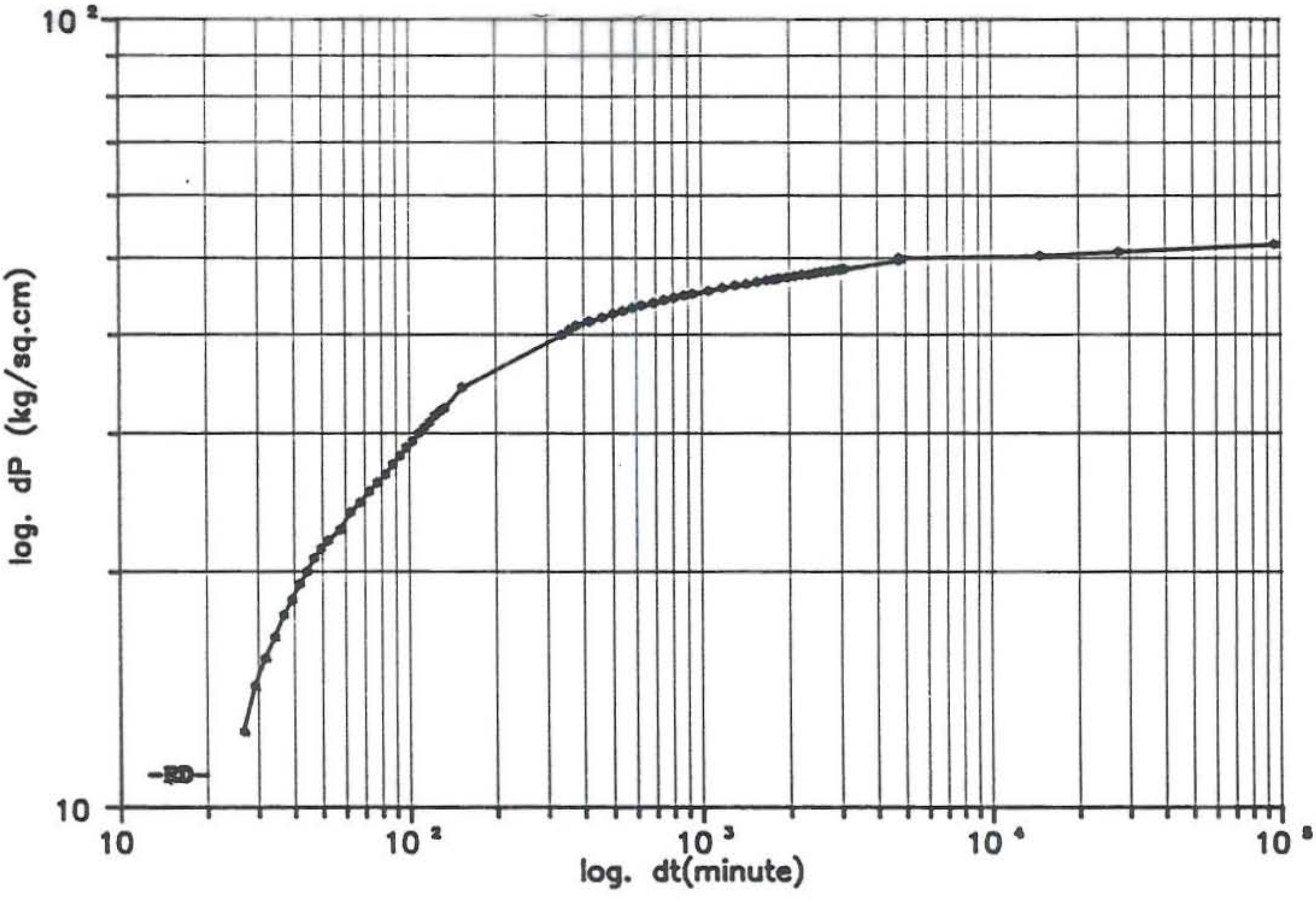

Figure. 14 Pressure recovery KhG-1, on log-log scale at 1400 m.

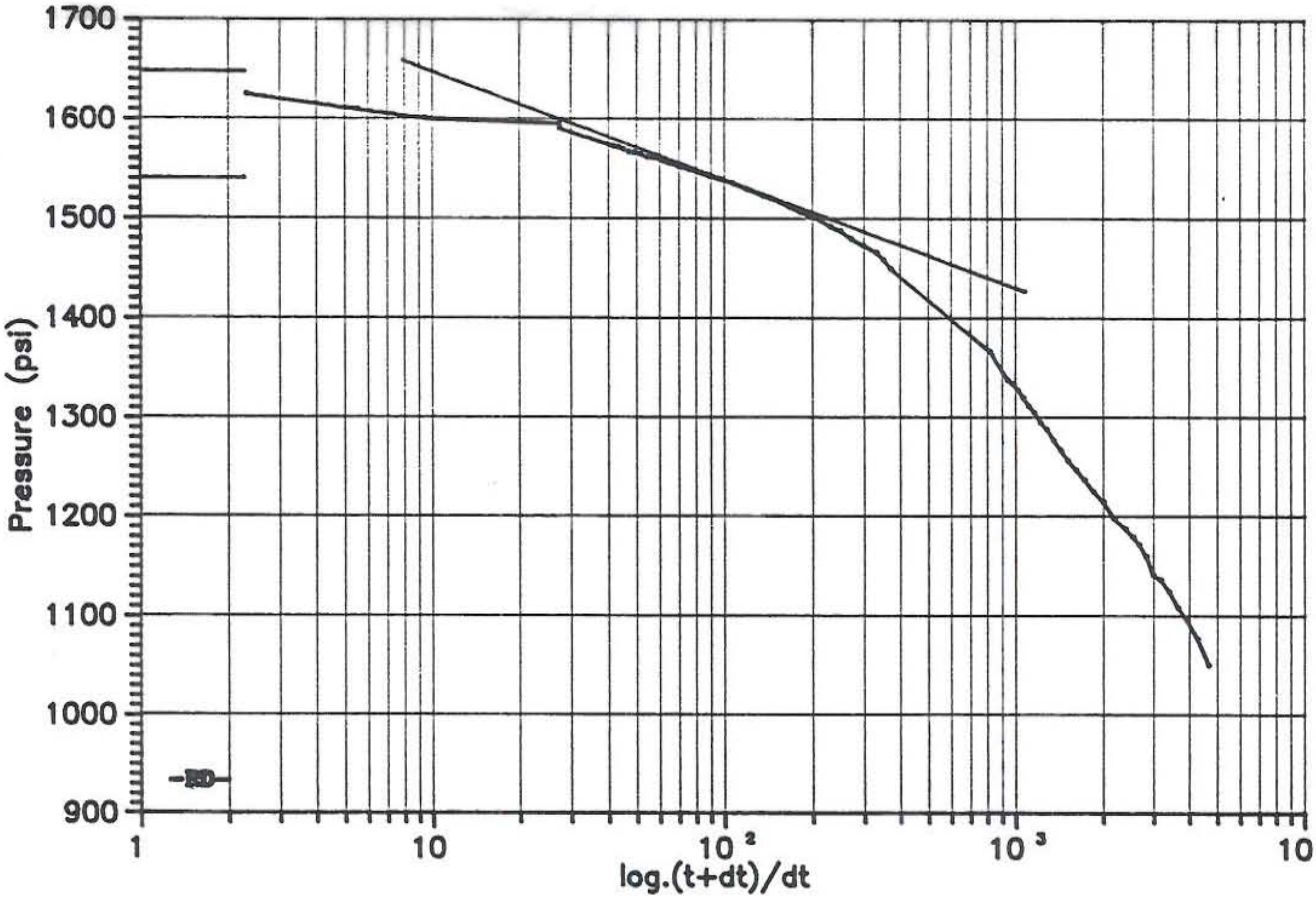

Figure. 15 Pressure recovery KhG-1, on Horner plot at 1400 m.

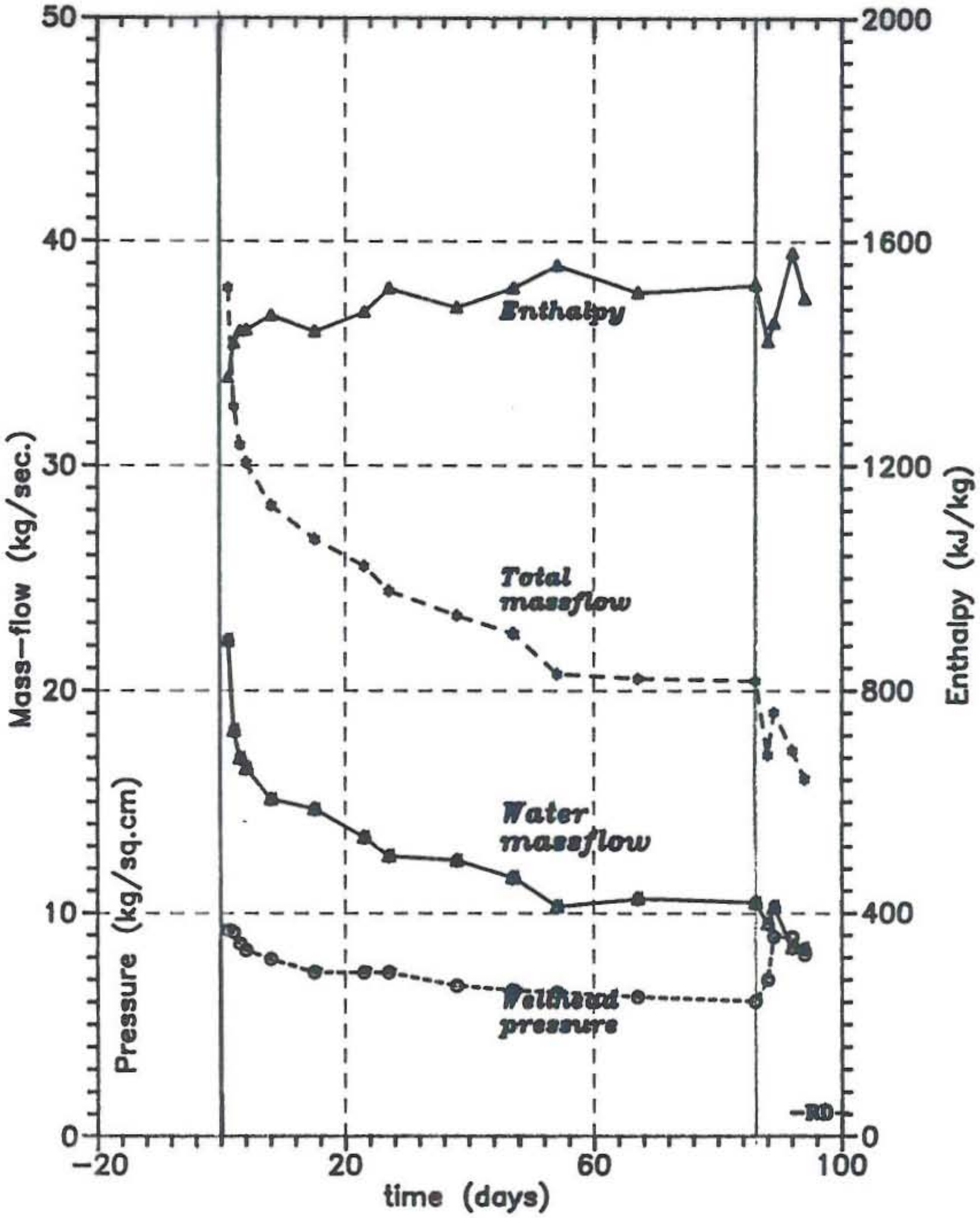

Figure. 16 Kolviðarholl KhG-1; Time Vs Enthalpy, massflow & W.H.P.

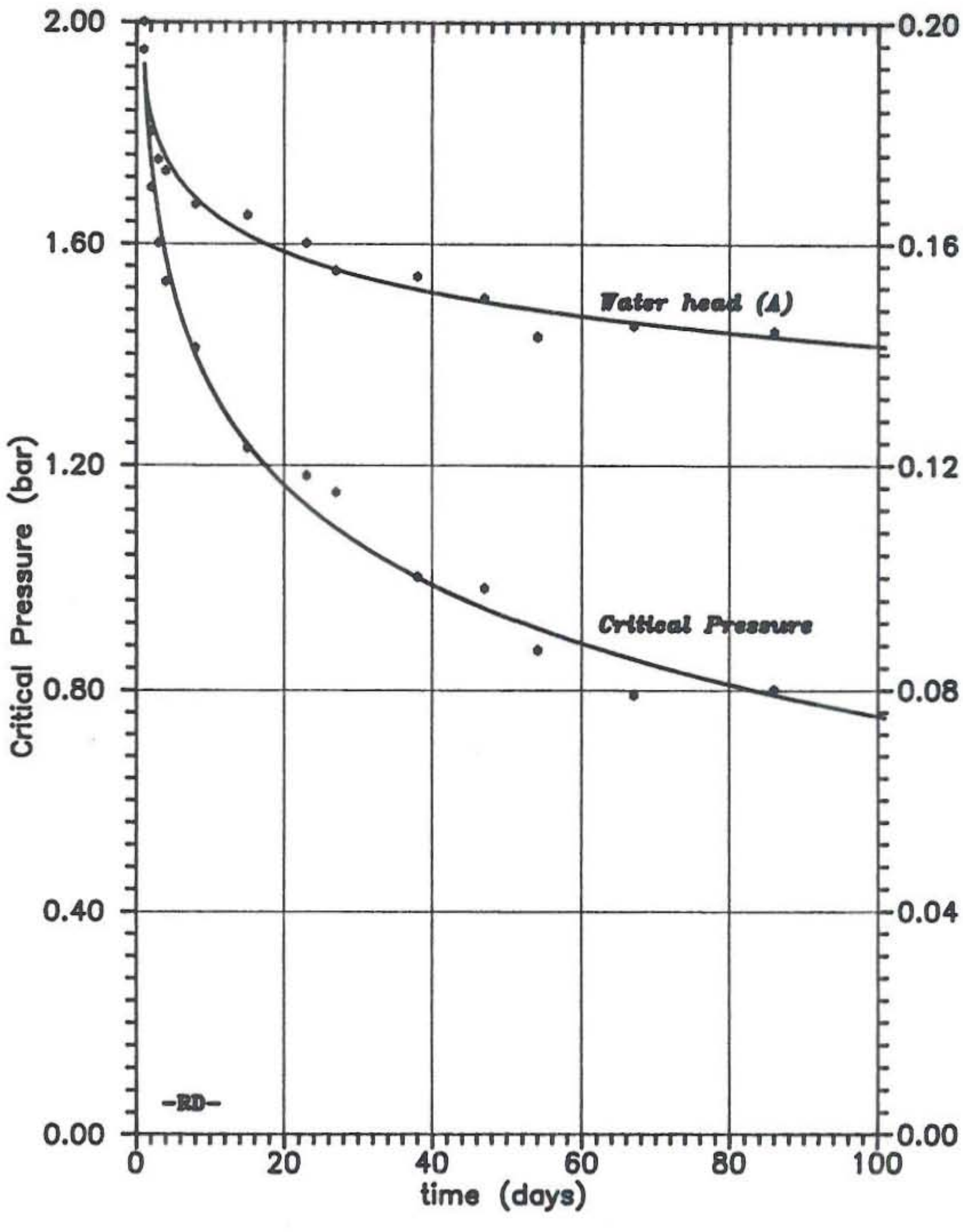

Figure. 17 Kolviðarholl KhG-1; Critical pressure and Water head in Weir box vs Time.

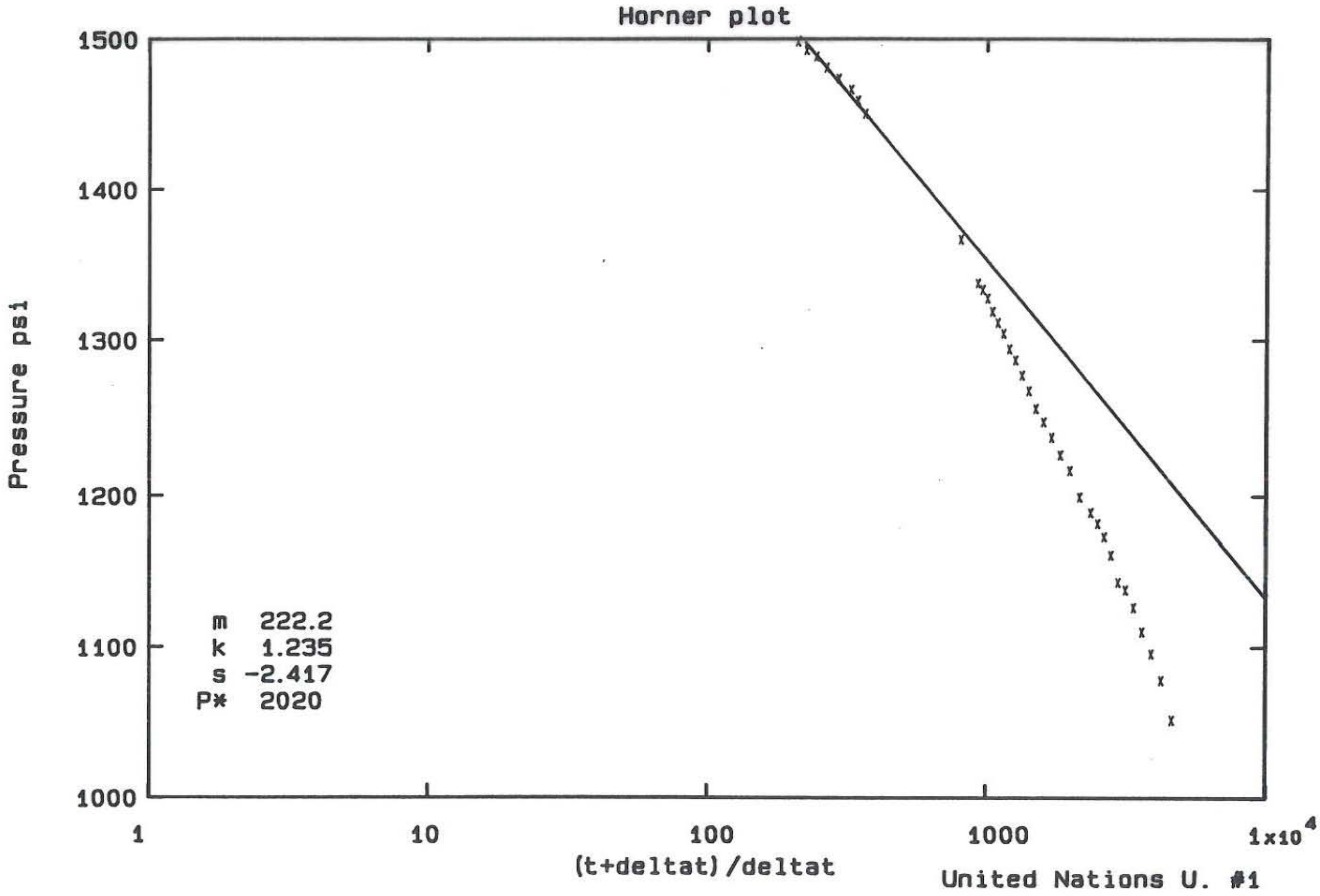

Figure. 18 KhG-1 /Early data- Horner plot.

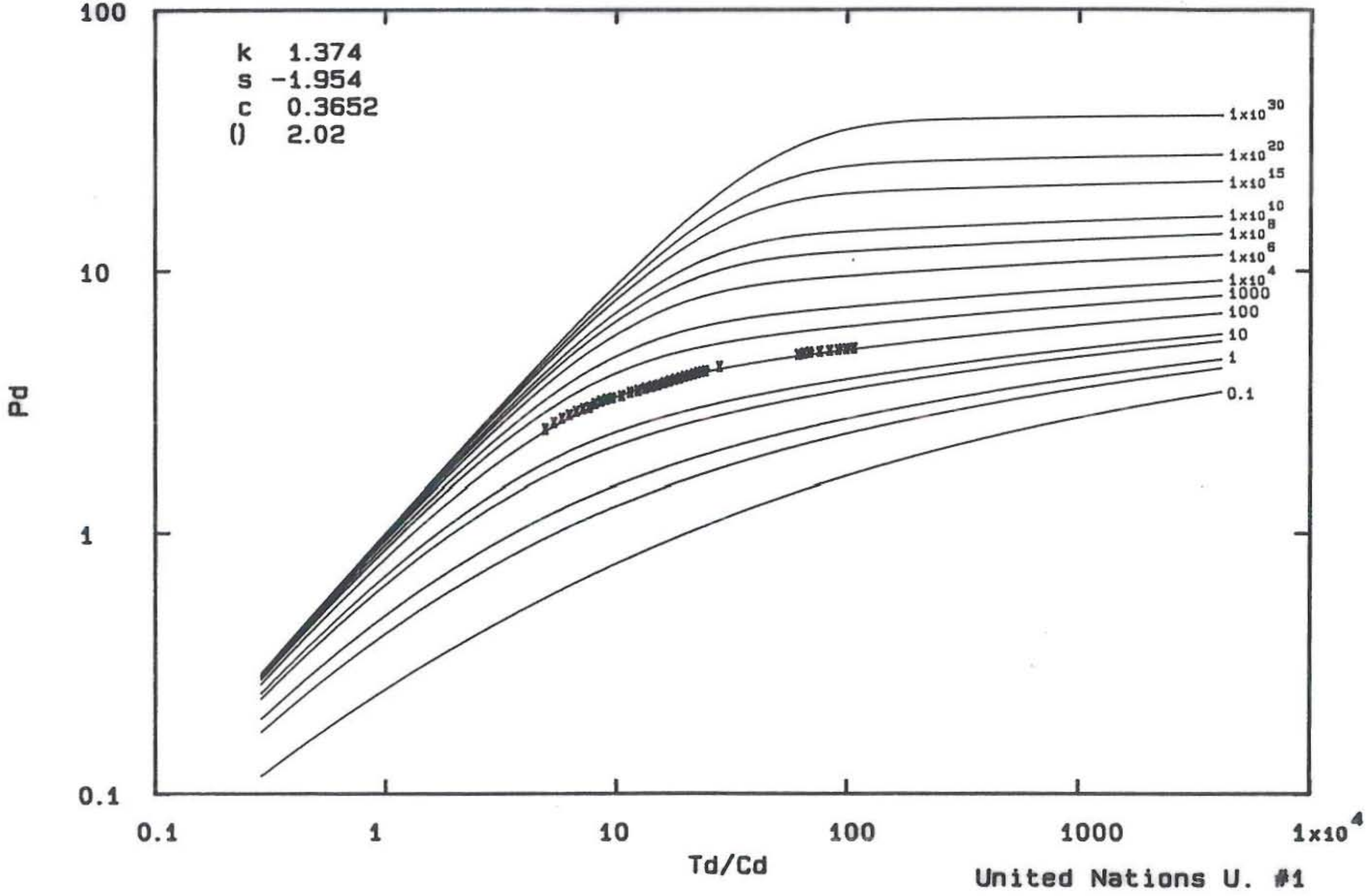

Figure. 19 KhG-1 /Early data- Storage & skin.

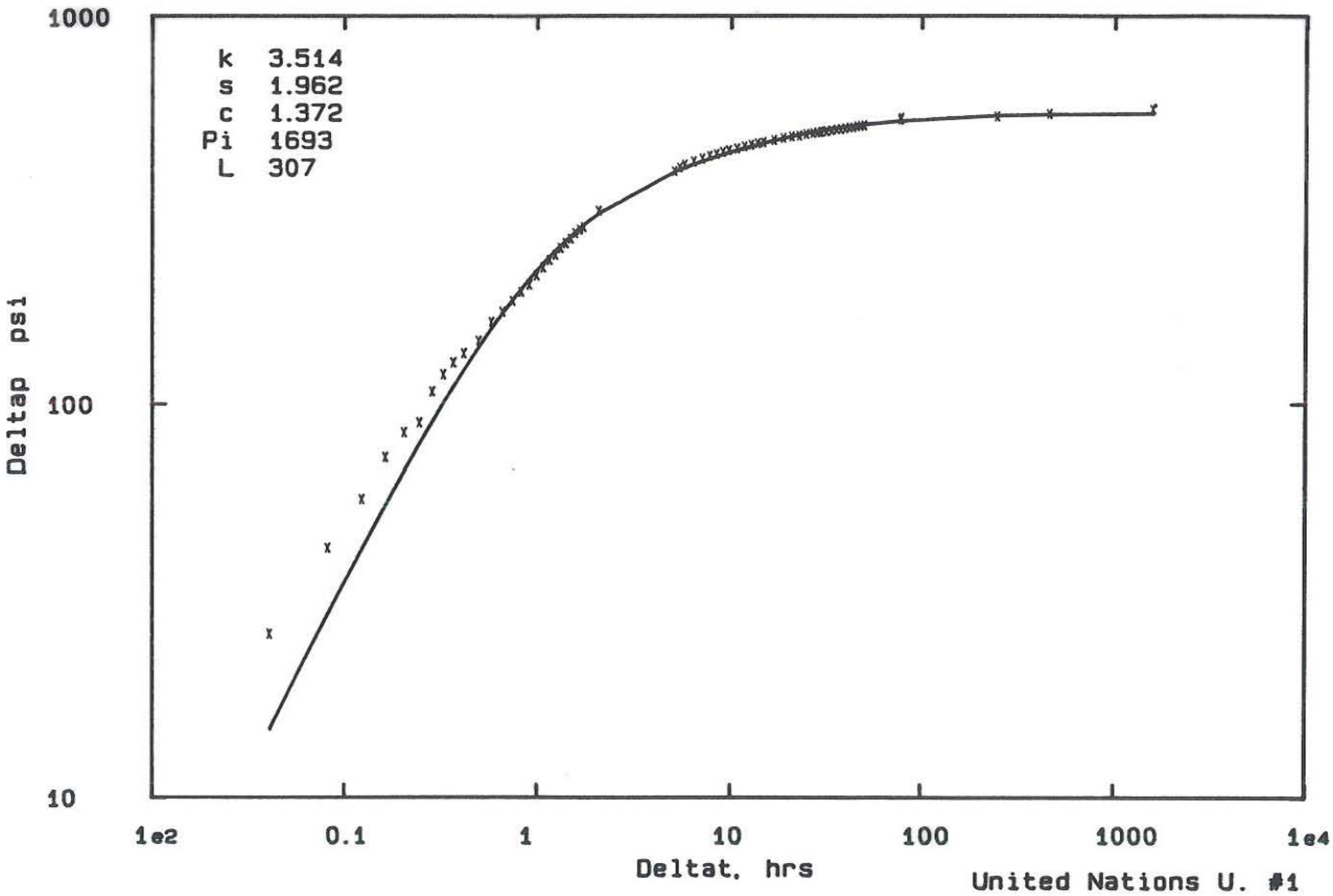

Figure. 20 KhG-1 /All data- Log-log plot match.

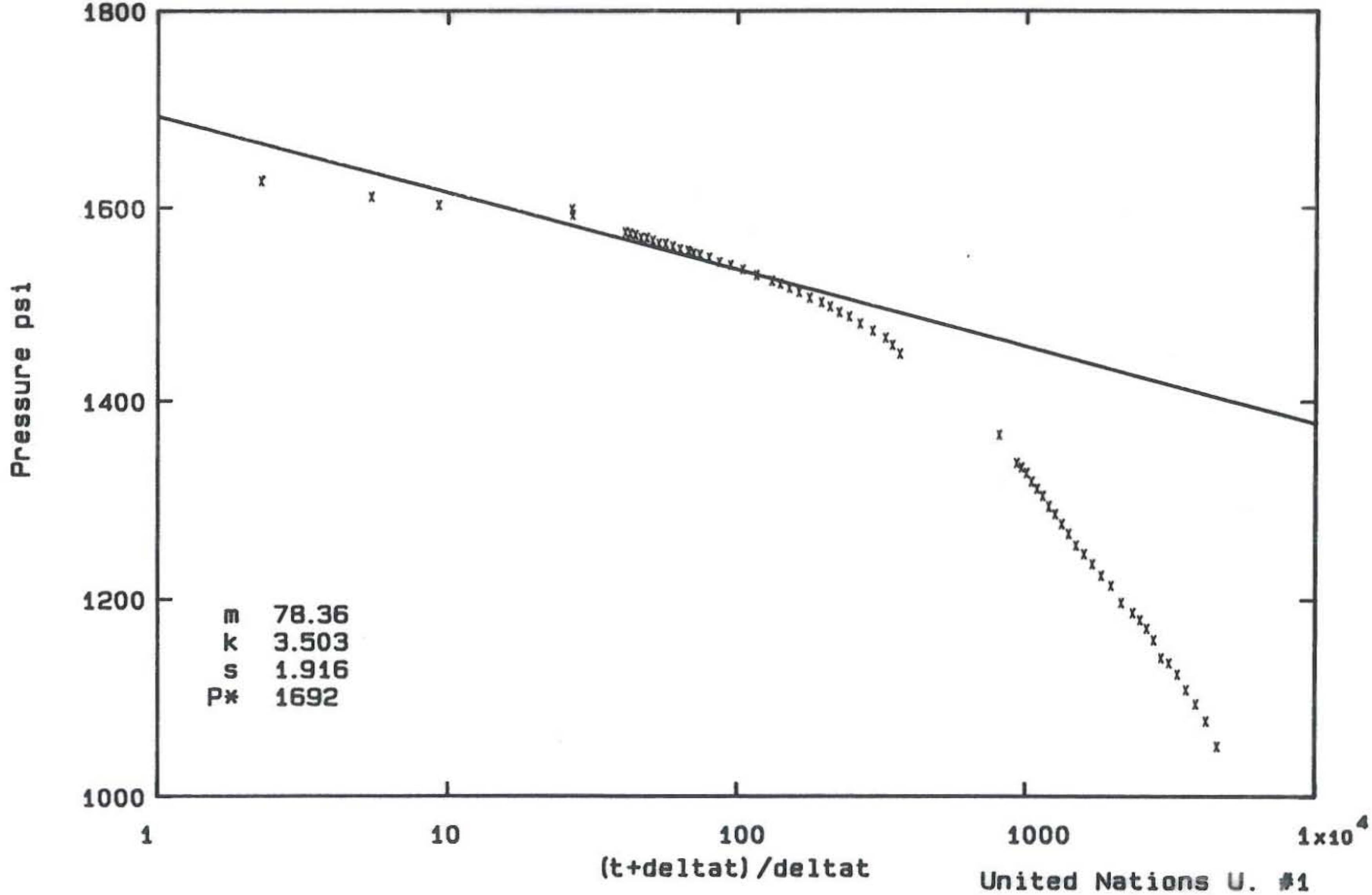

Figure. 21 KhG-1 /All data- Horner plot.

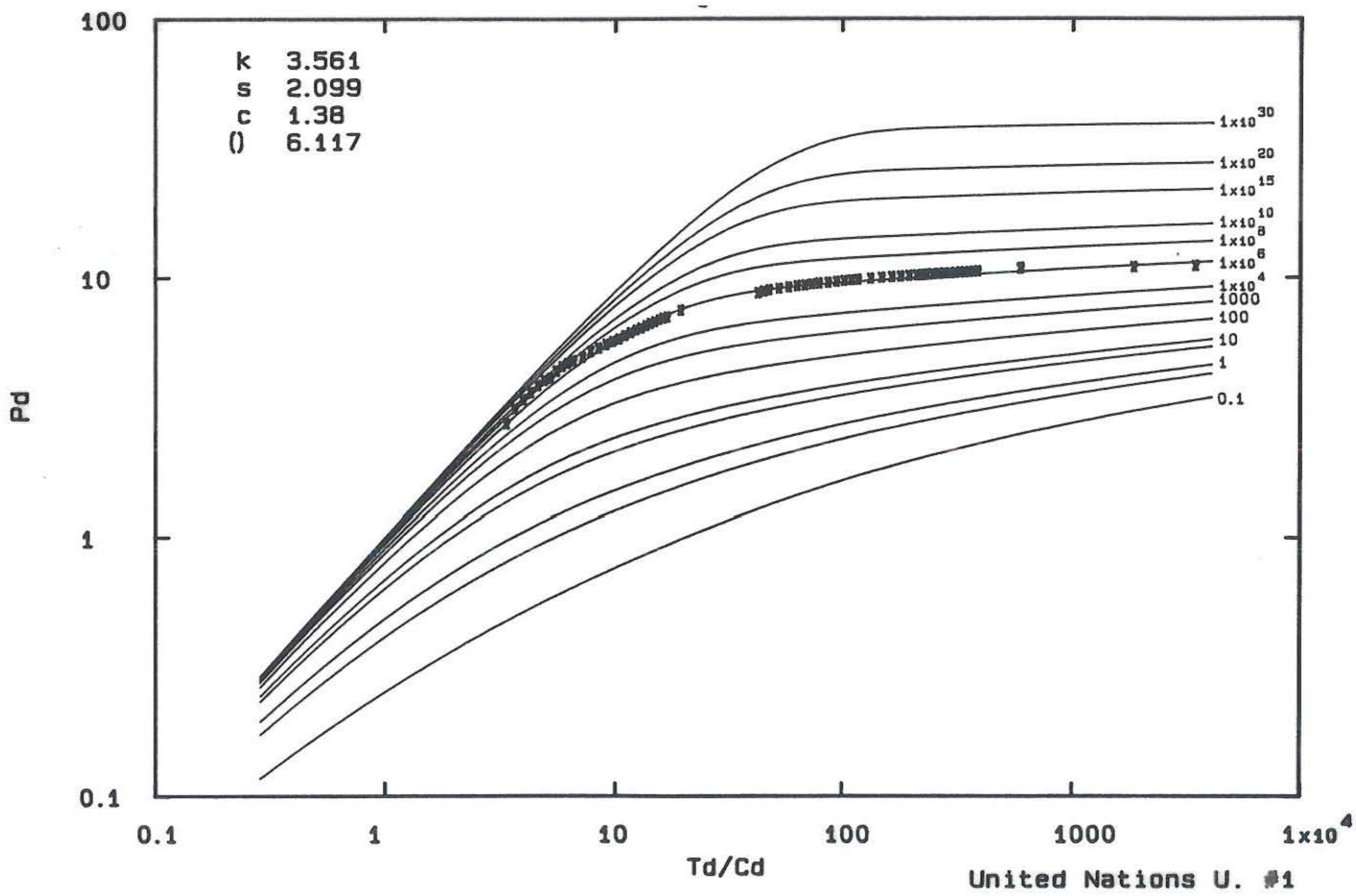

Figure. 22 KhG-1 /All data- Storage & skin.

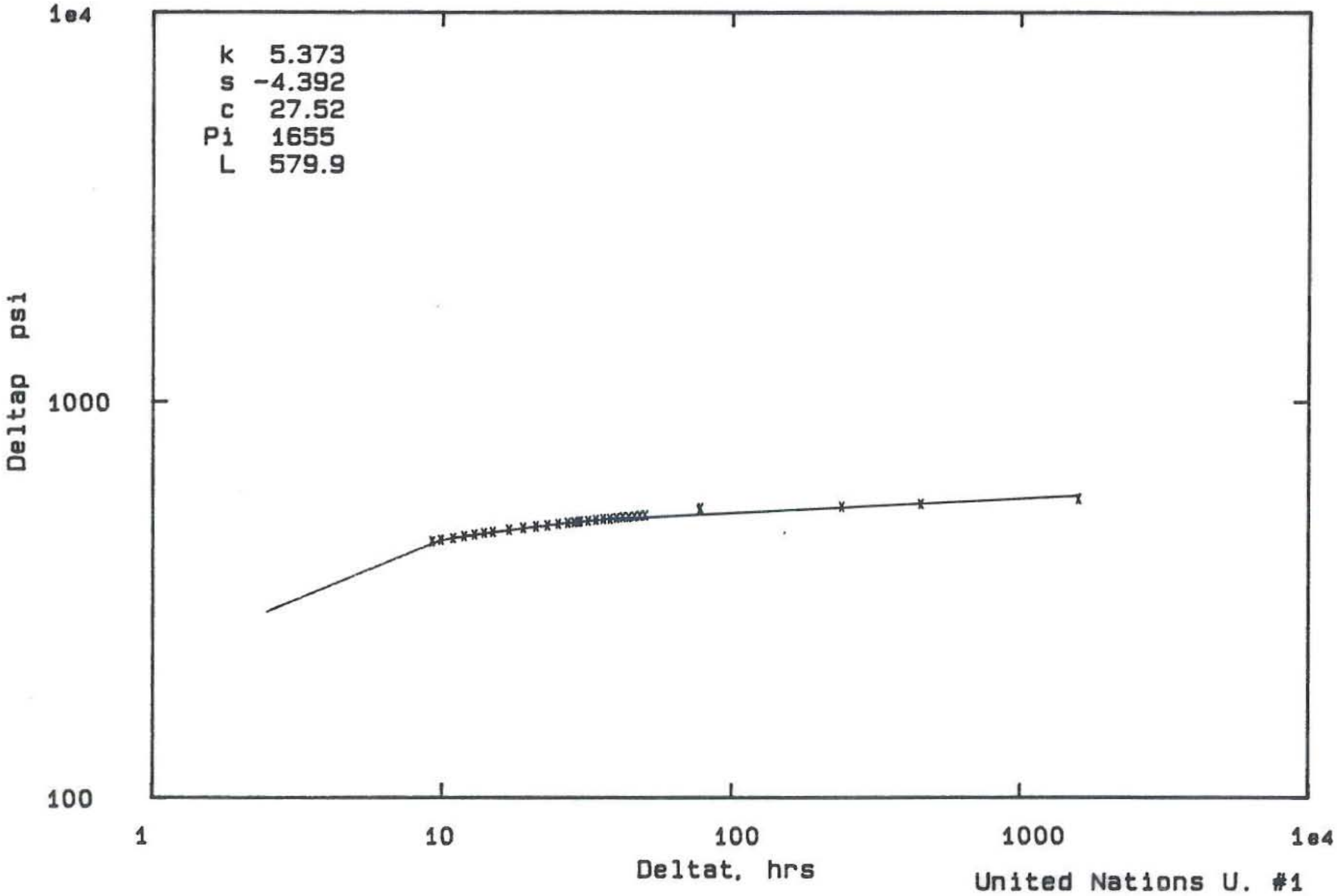

Figure. 23 KhG-1 /Late data- Log-log plot match.

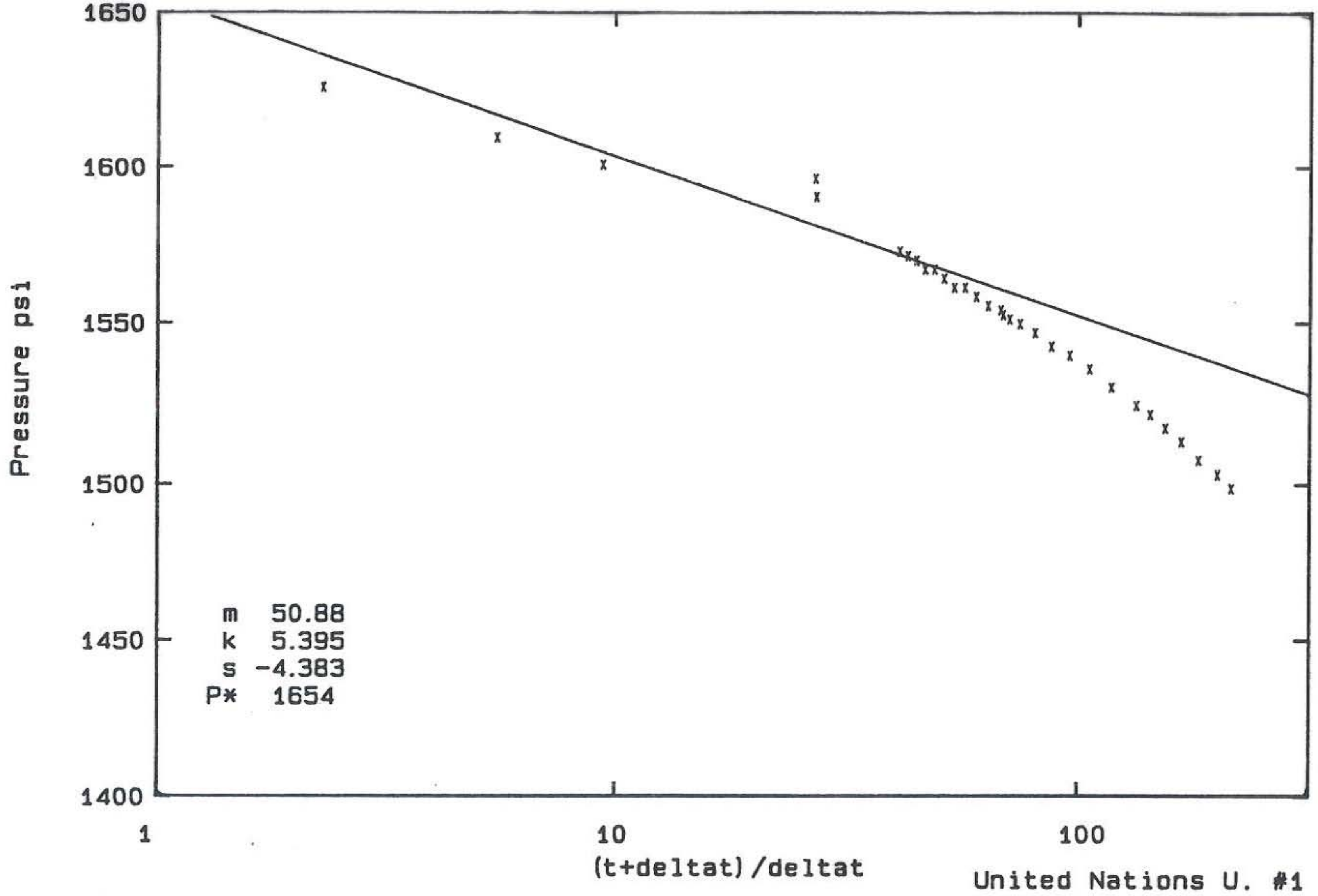

Figure. 24 KhG-1 /Late data- Horner plot.

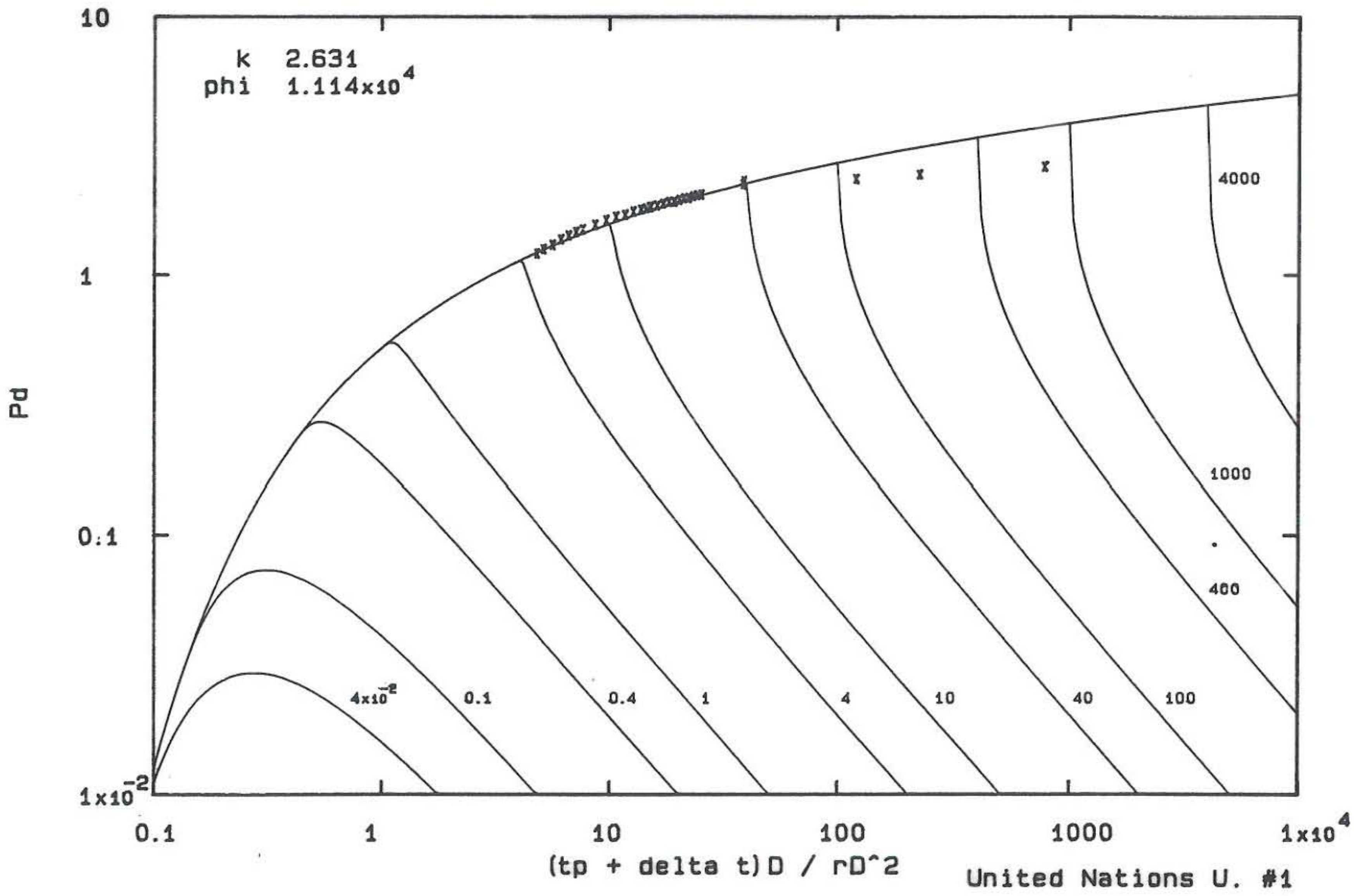

Figure. 25 KhG-1 /Late data- Line source solution.

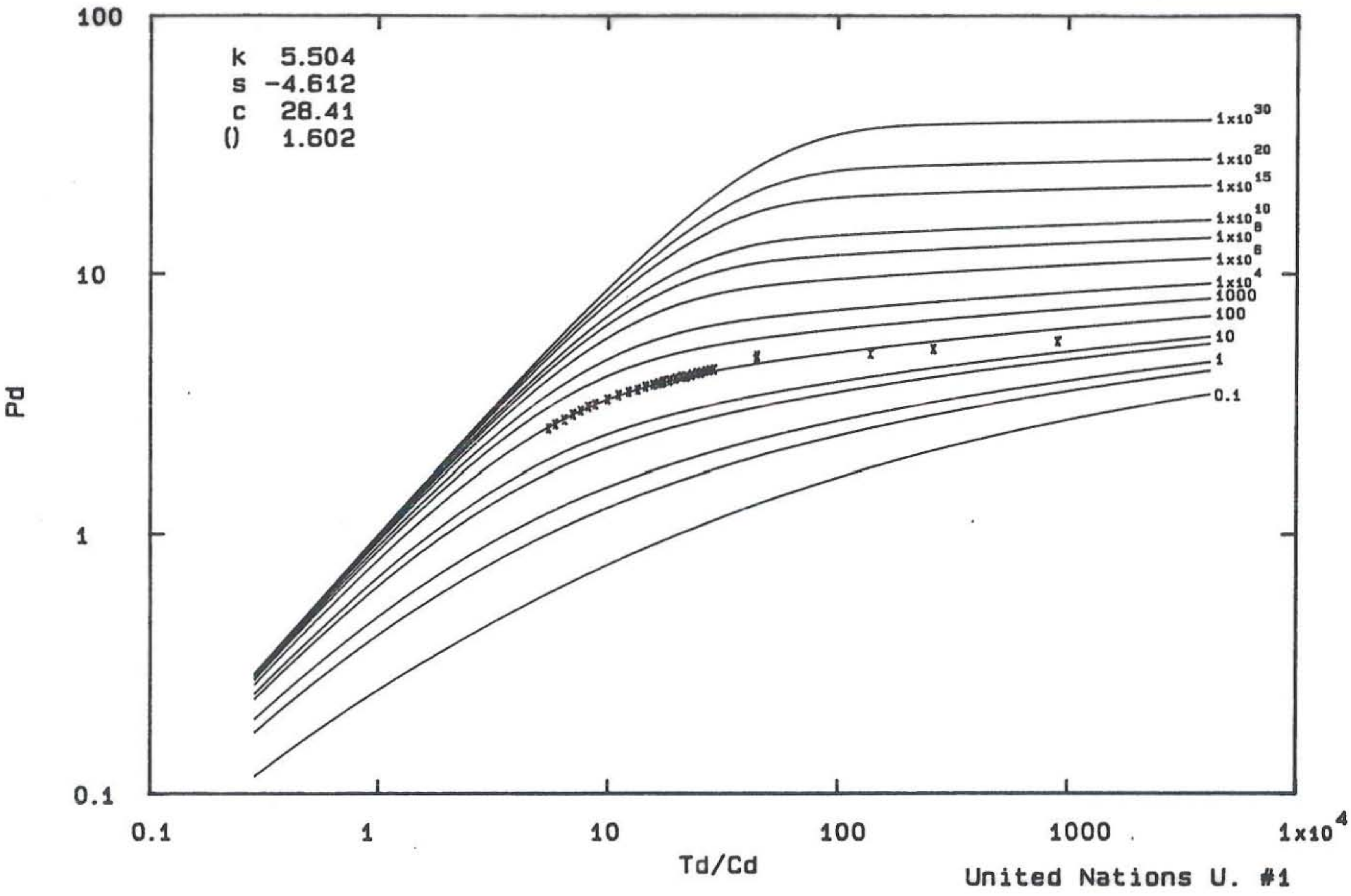

Figure. 26 KhG-1 /Late data- Storage & skin.